

**Final Research Report**  
Contract T1805, Task 22  
Cellular Automata

**A Cellular Automata Model for  
Use with Real Freeway Data**

by

Daniel J. Dailey and Nancy Taiyab  
**ITS Research Program**  
University of Washington  
Department of Electrical Engineering  
Seattle, Washington 98195

**Washington State Transportation Center (TRAC)**  
University of Washington, Box 354802  
University District Building, Suite 535  
1107 N.E. 45th Street  
Seattle, Washington 98105-4631

Washington State Department of Transportation  
Technical Monitor  
Pete Briglia  
ITS Program Manager

Sponsored by  
**Washington State**  
**Transportation Commission**  
Department of Transportation  
Olympia, Washington 98504-7370

in cooperation with  
**U.S. Department of Transportation**  
Federal Highway Administration

June 2002



## TECHNICAL REPORT STANDARD TITLE PAGE

1. REPORT NO. <b>WA-RD 537.1</b>	2. GOVERNMENT ACCESSION NO.	3. RECIPIENT'S CATALOG NO.	
4. TITLE AND SUBTITLE <b>A CELLULAR AUTOMATA MODEL FOR USE WITH REAL FREEWAY DATA</b>		5. REPORT DATE <b>June 2002</b>	
		6. PERFORMING ORGANIZATION CODE	
7. AUTHOR(S) <b>Daniel J. Dailey, Nancy Taiyab</b>		8. PERFORMING ORGANIZATION REPORT NO.	
9. PERFORMING ORGANIZATION NAME AND ADDRESS <b>Washington State Transportation Center (TRAC) University of Washington, Box 354802 University District Building; 1107 NE 45th Street, Suite 535 Seattle, Washington 98105-4631</b>		10. WORK UNIT NO.	
		11. CONTRACT OR GRANT NO. <b>Agreement T1803, Task 22</b>	
12. SPONSORING AGENCY NAME AND ADDRESS <b>Research Office Washington State Department of Transportation Transportation Building, MS 47370 Olympia, Washington 98504-7370 Gary Ray, Project Manager, 360-705-7975, rayg@wsdot.wa.gov</b>		13. TYPE OF REPORT AND PERIOD COVERED <b>Final Research Report</b>	
		14. SPONSORING AGENCY CODE	
15. SUPPLEMENTARY NOTES <b>This study was conducted in cooperation with the U.S. Department of Transportation, Federal Highway Administration.</b>			
16. ABSTRACT  <p style="text-align: justify;">The exponential rate of increase in freeway traffic is expanding the need for accurate and realistic methods to model and predict traffic flow. Traffic modeling and simulation facilitate an examination of both microscopic and macroscopic views of traffic flows and are therefore considered one of the most important analytical tools in traffic engineering. This report presents a cellular automata model for traffic flow simulation and prediction (CATS). Cellular automata models quantize complex behavior into simple individual components. In this model, the freeway being simulated is discretized into homogeneous cells of equal length, and time is discretized into timesteps of equal duration. The CATS model allows users to define locations within the road topology where volume and density data will be calculated so that the model results can be compared to observed highway data.</p>			
17. KEY WORDS <b>cellular automata, traffic modeling, dynamic simulation, prediction, control, ramp metering</b>		18. DISTRIBUTION STATEMENT <b>No restrictions. This document is available to the public through the National Technical Information Service, Springfield, VA 22616</b>	
19. SECURITY CLASSIF. (of this report)  <b>None</b>	20. SECURITY CLASSIF. (of this page)  <b>None</b>	21. NO. OF PAGES	22. PRICE



## **DISCLAIMER**

The contents of this report reflect the views of the authors, who are responsible for the facts and accuracy of the data presented herein. The contents do not necessarily reflect the official views or policies of the Washington State Transportation Commission, Department of Transportation, or the Federal Highway Administration. This report does not constitute a standard, specification, or regulation.



# TABLE OF CONTENTS

<b>DISCLAIMER</b> .....	<b>i</b>
<b>EXECUTIVE SUMMARY</b> .....	<b>1</b>
<b>1. INTRODUCTION</b> .....	<b>3</b>
1.1 MOTIVATION AND RESEARCH OBJECTIVE.....	3
1.2 LITERATURE OVERVIEW .....	4
1.2.1 <i>Traffic Model Classifications</i> .....	4
1.2.2 <i>Description of and Comparison to Existing Traffic Simulation Models</i> .....	5
1.2.3 <i>Explanation of Cellular Automata</i> .....	8
1.2.4 <i>Validation and Verification Methods</i> .....	8
1.3 REPORT OUTLINE .....	10
<b>2. MODEL DESCRIPTION</b> .....	<b>12</b>
2.1 SIMULATION SETUP.....	12
2.1.1 <i>Road Topology</i> .....	12
2.1.2 <i>Vehicle Description</i> .....	13
2.1.3 <i>Input Data</i> .....	14
2.2 MODELS FOR VEHICLE MOTION .....	14
2.2.1 <i>Model for Optimal Headway</i> .....	15
2.2.2 <i>Model for Speeding</i> .....	16
2.2.3 <i>Model for Breaking</i> .....	17
2.2.4 <i>Model for Lane Changing</i> .....	18
2.2.5 <i>Model for Upstream Effect of Ramps</i> .....	21
2.3 ALGORITHM FOR UPDATING VEHICLE POSITION .....	21
2.3.1 <i>Determine Vehicle Motion Goal</i> .....	22
2.3.2 <i>Optimal Headway Goal</i> .....	22
2.3.3 <i>Desired Speed Goal</i> .....	24
2.4 OUTPUT DATA .....	24
<b>3. CASE STUDY</b> .....	<b>28</b>
3.1 SIMULATION SETUP.....	28

3.1.1	<i>Road Topology</i> .....	28
3.1.2	<i>Vehicle Description</i> .....	30
3.1.3	<i>Simulation Time Period</i> .....	31
3.1.4	<i>Input Data from Roadway</i> .....	31
3.2	ANALYSIS OF FIELD DATA .....	31
3.2.1	<i>Traffic Count Analysis</i> .....	32
3.2.2	<i>Level of Service Analysis</i> .....	32
3.3	METHODS OF COMPARISON.....	35
3.3.1	<i>Conservation of Cars</i> .....	35
3.3.2	<i>Traffic Flow versus Density Plots</i> .....	36
3.4	PERFORMANCE OF THE CATS MODEL.....	38
3.4.1	<i>System Model</i> .....	38
3.4.2	<i>Calibration of Model for Optimal Headway</i> .....	39
<b>4.</b>	<b>CONCLUSIONS AND FUTURE WORK</b> .....	<b>46</b>
	<b>REFERENCES</b> .....	<b>49</b>
	<b>APPENDIX A</b> .....	<b>52</b>



## LIST OF FIGURES

Figure 1: Comparison of flow versus density plots for a) Field data and b) Simulation Results for a German Highway. [14].....	10
Figure 2: Piecewise linear model for optimal headway. ....	16
Figure 3: Shape of probability functions in the speeding model.....	17
Figure 4: Update of vehicles in same lane. ....	19
Figure 5: Update of vehicles when changing lanes.....	20
Figure 6: Block diagram for CATS vehicle update algorithm.....	23
Figure 7: Flow chart for vehicle update algorithm. (a) Determine the goal of vehicle motion.	25
Figure 7 (continued): Flow chart for vehicle update algorithm. (b) Determine desired speed. ...	26
Figure 7 (continued): Flow chart for vehicle update algorithm. (c) Apply lane changing model to update vehicle position.....	27
Figure 8: I-5 freeway section used in case study.....	29
Figure 9: Percentage of speeding vehicles on the roadway .....	30
Figure 10: Level of service distribution by lane using volume data from sensors in the roadway. ....	34
Figure 11: Theoretical relationship between traffic flow and density and illustration of levels of service.....	37
Figure 12: System model for CATS and roadway. ....	38
Figure 13: Comparison of conservation of cars between model and field data using different values for input parameters in the model for optimal headway. ....	40
Figure 14: Flow versus density plots for varying $S_R$ values.....	41
Figure 14 (continued): Flow versus density plots for varying $S_R$ values. ....	42
Figure 14 (continued): Flow versus density plots for varying $S_R$ values. ....	43
Figure 15: Maximum density versus flow for each $S_R$ value.....	44
Figure 16: Random component of $\delta$ versus $S_R$ with polynomial best fit curve.....	45
Figure 17: Flow versus density plot for optimal $S_R$ value. ....	45

## LIST OF TABLES

Table 1: Levels of service definition for freeway sections. ....	31
--	----



## **EXECUTIVE SUMMARY**

There are large potential benefits to a variety of traffic information and management activities if accurate traffic condition prediction can be done over a large region. Changes to geometry, as well as congestion, can be simulated using the proposed technique so that arenas ranging from planning to traveler information can benefit. For example, the types of planning questions that might benefit from such modeling are as broad as the effect of lane closures for maintenance, the time of day for such maintenance, to changes in HOV policy or incident response resource allocation. The traveler information benefits range from prediction for route decisions to estimates of incident clearing times. The accurate prediction of detailed traffic behavior opens the door to a new genre of route guidance, fleet management, and transit management and advance traveler information systems possibilities on a regional and national scale.

Creating a model that accurately predicts future congestion based on the physics of traffic provides a foundation for real-time, optimal control as well as providing a powerful test bed for modeling roadway capacity changes, such as lane closures and incidents. This proof of principle activity on I-5 North can contribute a predictive capability to the ramp control activity already underway at WSDOT TSMC, as well as providing the framework for a combined freeway and arterial control system.

This report presents a model for traffic flow simulation and prediction. The model uses cellular automaton theory to model complex traffic behavior. The advantage of the cellular automata approach is that the roadway to be modeled is quantized into simple homogeneous cells, time is quantized into discrete steps, and physical quantities take on a finite set of values. Also, the state of the cells is updated at discrete timesteps by using a vehicle update algorithm that combines a few vehicle motion models that are governed by a relatively small set of parameters. This allows the model to be calibrated easily and also allows the simulation to run very fast. CATS can simulate traffic flow on the road in under 2 percent of the actual time period being simulated.

Using volume data from traffic sensors embedded in the access and exit ramps of the highway as boundary conditions, the model predicts traffic flow on the mainlines at points farther downstream. To evaluate the accuracy of CATS, the observed volume and occupancy measures can be compared directly with field data from traffic sensors on the road. The extensive

comparison of the calculated results with field data is one of the key difference between CATS and existing models.

To evaluate the model's performance, it is used to simulate southbound traffic on an 11-mile section of I-5 in Seattle, Washington. A simulation period that covered a broad range of traffic conditions was chosen to ensure that the model was being tested for all levels of congestion. A method parameter calibration was presented, using the model for optimal headway as an example. This model was chosen because it has the greatest impact on the vehicle position update algorithm. CATS was run repeatedly for the same simulation period and roadway using different values of input parameters. The results from the model were evaluated with a conservation of cars metric and plots of traffic flow versus density. These metrics were compared, and the best values for the input parameters were chosen accordingly. The comparison showed that running CATS with these input parameter values did indeed increase the accuracy of the model and that CATS was able to accurately predict vehicle behavior on the freeway.

## **1. INTRODUCTION**

The exponential rate of increase in freeway traffic is driving expanding the need for accurate and realistic methods to model and predict traffic flow. Traffic modeling and simulation facilitates an examination of both microscopic and macroscopic views of traffic flows and is therefore considered one of the most important analytical tools in traffic engineering.

### ***1.1 MOTIVATION AND RESEARCH OBJECTIVE***

Accurate mathematical and computer models of traffic flow are used to understand aggregate traffic behavior, design efficient traffic control and management strategies, assess and optimize the impacts of roadway geometries, and design new highway lanes [1].

This report presents a cellular automata model for traffic flow simulation and prediction (CATS). Cellular automata models quantize complex behavior into simple individual components. In this model, the freeway being simulated is discretized into homogeneous cells of equal length, and time is discretized into timesteps of equal duration. These cells can be either in an occupied or empty state, depending on whether a vehicle is present at that location. The state of the cells is updated sequentially at each time step with a set of vehicle position update rules and real-time volume data sampled from embedded inductance loop traffic sensors on the access and exit ramps of the freeway. These volume data are used to determine the number of vehicles entering and exiting the freeway at each timestep. The vehicle position update rules apply to vehicles already on the freeway. These rules include a car-following optimal-headway model, a model for speeding, a model for braking, a model for lane changing, and a model for the upstream effect of access and exit ramps. Each of these motion models has a set of input parameters that governs its behaviour. These parameters can be adjusted to improve the performance of the simulation model. The CATS model also allows users to define locations within the road topology where volume and density data will be calculated so that the model results can be compared to observed highway data. These locations usually correspond to the position of the embedded loop traffic sensors.

To observe the results of the CATS model when it is used to simulate real traffic, a case study was conducted on an 11-mile section of the I-5 freeway in Seattle over a 12-hour period. The actual traffic data provided by the embedded inductance loop traffic sensors on the freeway and the

model were compared by using both qualitative and quantitative measures. These included statistical conservation and correlation metrics and comparison of traffic flow versus density plots.

## **1.2 LITERATURE OVERVIEW**

Traffic models have historically been developed to address different traffic problems. In general, these models can be classified as either macroscopic, mesoscopic, or microscopic. This section outlines the basic characteristics of these model classifications followed by a description of the most widely used traffic simulation models and a comparison of these models to the CATS model presented in this report. These models include NETSIM (NETwork SIMulation), FRESIM (FREeway SIMulation), Daganzo's theoretical cell transmission model and its implementation (NETCELL), and Nagel and Schreckenberg's cellular automaton model. Both NETSIM and FRESIM are part of CORSIM (CORridor SIMulation), a microscopic corridor simulation model. Following this discussion, an explanation of cellular automata is given, and the measures used to verify and validate traffic models is described, along with examples taken from the literature.

### **1.2.1 Traffic Model Classifications**

Macroscopic models describe traffic with aggregate variables such as traffic density, mean speed, and volume. The use of such variables reduces the computation requirements for macroscopic modeling, making real-time calculation quite feasible. However, macroscopic models cannot estimate travel time, turning movements at intersections, fuel consumption, and control parameters on a short time scale [2].

Microscopic modeling considers the individual vehicle's physical status and the factors that control human driving behavior. The movement of individual vehicles is governed by the driver's behavior, the road topology, the status of surrounding vehicles, and the headway distribution. Each vehicle in the traffic may be described by a set of parameters that includes position, actual speed, desired speed, route choice, and willingness to pass the other vehicles. It is very difficult to derive analytic and deterministic equations to precisely describe microscopic traffic phenomenon and quantify all the factors that control human driving behavior. Therefore, computer-based simulations are preferred over analytic models in this case. However, computational complexity increases rapidly with the number of vehicles being considered, and therefore, real-time simulation requires a trade off between complexity and computation costs.

Mesoscopic models represent a compromise between the accuracy of a microscopic model and the computational efficiency of a macroscopic model. These models are often used when real-time simulation with a high level of detail is needed [3].

### ***1.2.2 Description of and Comparison to Existing Traffic Simulation Models***

NETSIM [4, 5] is a microscopic urban traffic simulation model developed by the U.S. Federal Highway Administration (FHWA). It is capable of simulating a variety of operational conditions experienced in an urban street network environment. The road topology in this model is represented as a network of nodes and unidirectional links. The links represent urban streets or freeway sections, and the “nodes represent urban intersections or points at which a geometric property changes (e.g., a lane drop, a change in grade, or a major midblock traffic generator).” [4] This model “identifies each vehicle by category (e.g., auto, carpool, truck, or bus) and by type and also assigns a driver-behavioural characteristic (passive or aggressive) to each vehicle.” [4] Each vehicle is viewed as an individual entity whose position must be updated every second. The effect of pedestrian traffic (which can delay vehicles at intersections) is also considered in the simulation because the road topology includes arterial roads and intersections. In addition, NETSIM distinguishes between public and private vehicles. Both types of vehicles have to adhere to traffic control devices such as stoplights, but public vehicles such as buses also have to service passengers at bus stops. In comparison, CATS is used solely to simulate freeway traffic. Therefore, whereas it does distinguish vehicle by type, it does not classify private and public vehicles separately and does not consider the effects of pedestrian traffic since on a freeway both buses and cars behave similarly and there is no pedestrian traffic. Also, CATS does not make any assumptions about the drivers of the individual vehicles and introduces differences in driving goals through probabilistic speeding and lane changing models.

FRESIM, [4, 6] the complement of NETSIM, is the most detailed and powerful microscopic freeway corridor simulation model developed by the FHWA. The road topology is defined in a manner similar to that of NETSIM. However, FRESIM has support for more detailed topological features, variations in grade, radius of curvature, and superelevation on the freeway. Vehicle types are assigned stochastically with a vehicle type distribution defined by the user, and they are released into the road through mainline entry points and on ramps and removed from the exit ramps, in a manner similar to the CATS model. One key difference between FRESIM and CATS,

however, is that the FRESIM model determines the number of vehicles to be introduced into the road via a probability distribution based on traffic volumes provided by the user, whereas CATS uses real volume data taken from embedded traffic sensors in the freeway. FRESIM uses car following and lane changing models to determine the vehicle position at each step, can simulate ramp metering, and allows the user to define incidents by lane. CATS also includes similar models in its vehicle position update algorithm and allows users to define incidents by lane, but it is not able to simulate ramp metering at this time. In addition, both FRESIM and CATS allow users to define loop locations where traffic measures such as volume, occupancy, and speed must be calculated to facilitate comparison between simulated and actual data.

The cell transmission model developed by Carlos Daganzo [3, 7, 8] at the University of California, Berkeley, is a mesoscopic traffic flow model. It is classified as such because it moves vehicles on the basis of averaged macroscopic conditions, but the cell size can be small enough to capture the microscopic state of individual vehicles. This model is the discrete equivalent of the hydrodynamic model introduced by Lighthill and Whitham in 1955 and Richards in 1956 [3]. “According to this model, traffic is described as fluid with relationships between flow, concentration and speed,” [3] and the model assumes density and traffic flow to be continuous variables. The implementation of this model is NETCELL [9], a freeway network simulation package written in C. NETCELL represents the road topology by a series of cells and arcs. A cell represents the distance traveled by a typical vehicle under free flow conditions in one timestep, and an arc represents a homogeneous roadway segment without any entrances or exits [9]. In comparison, CATS allows the user to define the cell length, making it possible for cars to traverse many cells in one timestep, depending on the speed of the car and the length of the cell. Daganzo’s model determines vehicle motion by using two fundamental parameters: the maximum number of vehicles that can occupy a cell and the maximum number of cars that can flow into a cell in one timestep. This means that a cell can hold multiple vehicles at one timestep, as opposed to the one-car maximum imposed by the CATS model. The boundary conditions in Daganzo’s model are specified by input and output cells that have special parameters. For example, the input cell can have an infinite number of cars flowing into it in a single timestep. Merging junctions are represented by a special merging cell and two upstream cells. Similarly, a diverging junction is modeled by a diverging cell and two downstream cells. The input parameters to the model include routing information, origin-destination pairs for the vehicles, and location and time of traffic



incidents. NETCELL associates an origin-destination pair with each vehicle so the path of each individual car can be tracked. In comparison, the road topology in CATS is discretized into homogeneous cells, and the merging and diverging junctions are modeled by access and exit ramps. Also, CATS does not track the path of individual vehicles, preferring to view the traffic flow as an aggregate process. Another significant difference between NETCELL and CATS lies in the nature of cell update. NETCELL updates cells in any order by recursively computing the vehicle occupancy of every cell at each timestep, whereas CATS needs to update cells in a lane by lane downstream order to ensure that the vehicle position update rules can be applied correctly.

The cellular automaton model for freeway traffic developed by Kai Nagel and Michael Schreckenberg [10, 11, 12, 13, 14, 15] is the one that is most similar to the CATS model. The road topology in this model is represented by a one-dimensional cell lattice, as it is in CATS, with each cell belonging to one of two possible states (occupied or empty). This model is used to simulate traffic with either periodic or open road boundary conditions. A road with periodic boundary conditions is one where cars travel in a circle and cannot enter or exit, similar to a racetrack. A road with open boundary conditions has entry and exit points at defined locations, similar to a freeway with access and exit ramps [13]. The CATS model is used primarily to simulate road sections with open boundary conditions. The Nagel-Schreckenberg model assigns each vehicle an integer velocity within a specified range. The vehicle position update at each time step is governed by acceleration, deceleration car motion, and randomization rules. The acceleration/deceleration rule evaluates the current speed and headway to determine whether the speed can be increased without causing a collision or whether it needs to be decreased to avoid a collision. The car motion rule covers the default case in which the vehicle maintains its original speed and advances the appropriate number of cells. The vehicle's speed can also be decreased with a certain probability regardless of the traffic conditions, according to the randomization rule. This randomization is essential for ensuring that the model simulates realistic traffic flow. Otherwise, the traffic flow will be completely deterministic. Similarly, CATS considers the speed and headway of each vehicle to determine its motion and uses random numbers to introduce stochasticity into the model.

### ***1.2.3 Explanation of Cellular Automata***

Cellular automata were originally introduced by von Neumann and Ulam in the 1960s with the particular purpose of modeling biological self-reproduction [16, 17, 18]. Since then, they have been used broadly for physics applications such as particle transport simulations and thermodynamics studies. Creamer and Ludwig have used a cellular automaton model in the form of a Boolean simulation of traffic flow [19]. The Boolean model represents individual vehicles by 1-bit variables that are placed in computer memory locations analogous to the locations of vehicles on the roadway. Thus, the pattern of cars within a lane of a roadway, at a discrete time instant, is represented by a corresponding chain of logical 0's (representing free space) and 1's (marking the position of a vehicle). More recently, since the introduction of the Nagel-Schreckenberg model in 1992, cellular automata have become a well-established method of traffic flow modeling. "[The] comparatively low computational cost of CA models made it possible to conduct large-scale real-time simulations of urban traffic in the cities of Duisburg and Dallas/Fort Worth." [12, 20]

The traffic simulation model presented in this report is a minimally microscopic cellular automaton model. This means that both time and space are discrete variables, and physical quantities take on a finite set of discrete values. The roadway is represented by a uniform cell lattice in which each cell belongs to a discrete set of states. The state of the cells is updated at discrete timesteps with a set of update rules that combine a few vehicle motion models that are governed by a small set of parameters. "To have only a small set of parameters to calibrate as the CA can be a tremendous advantage when coping with complicated situations such as the lane changing behaviour, where it is difficult to calibrate the more complicated models." [15]

### ***1.2.4 Validation and Verification Methods***

The validation and verification of the results from traffic simulation models continue to be challenging because of the limited availability of real traffic data. An examination of past work shows that one of the key differentiating features of the CATS model is that CATS is used to simulate a real highway, and extensive real-time data are used to drive the model and verify the results.

Generally, two methods are used to test a traffic simulation model. First, the simulated data are compared to established theoretical results, and second, the simulated data are compared to real

data taken from the highway [21]. These comparisons can be done on both qualitative and quantitative levels.

The FHWA conducted a case study to test the FRESIM model on a 5-mile section of the I-5 freeway in Seattle, Washington [6]. To verify the results, the average speed values on the highway given by the model were compared with field data for a 15-minute period from 4:00 to 4:15 pm. This was a limited data set, given that traffic flows vary greatly over the course of the day, but as quoted from the document, “no further field observations of actual speeds/travel times were available to permit a comparison of the model to field data for periods other than 4:00 to 4:15 pm.” [6]

Aycin and Benekohal used FRESIM to simulate a portion of the I-71 freeway in Columbus, Ohio [22]. They evaluated the performance of FRESIM qualitatively by using regression analysis and quantitatively by comparing plots of average speed and density versus time from model and field data. However, “regression analysis between field data and simulation results for the car-following models did not provide meaningful results due to the correlation that exists between data points from the simulation and between data points from the field data.” [22] Therefore, they quantitatively analyzed performance by visually comparing plots of average speed and density versus time for the simulated and actual data for a period of 135 seconds.

The cell transmission model developed by Daganzo has not been tested with real data. “Field experiments are currently being planned to assess the accuracy of the model.” [7] Instead, Daganzo compares the results of simulations from the model with expected theoretical results by using a fictitious homogeneous section of highway with a large input flow and restricted steady output. The graphs of traffic flow versus time and traffic flow (vehicles/hour) versus traffic density (vehicles/ lane) are visually compared. These comparisons establish that the model “may have the potential for reproducing real-life phenomena but a very large empirical effort would be needed to pinpoint more precisely a ‘correct’ model.” [7]

The Nagel-Schreckenberg cellular automata model can be verified by using a road section with periodic boundary conditions [10]. Traffic is simulated on a closed, single-lane loop. This forces the number of cars in the model to remain constant because there are no access or exit points. The plot of traffic flow versus density, often referred to as the fundamental diagram, is plotted for both

simulated and observed results and compared visually [10, 14]. Figure 1 shows an example from Nagel et al. [14] in which the traffic flow versus density plots generated with field data from a German Highway (A6 Heilbronn-Nurnberg) and simulation results from the Nagel-Schreckenberg model are compared visually.

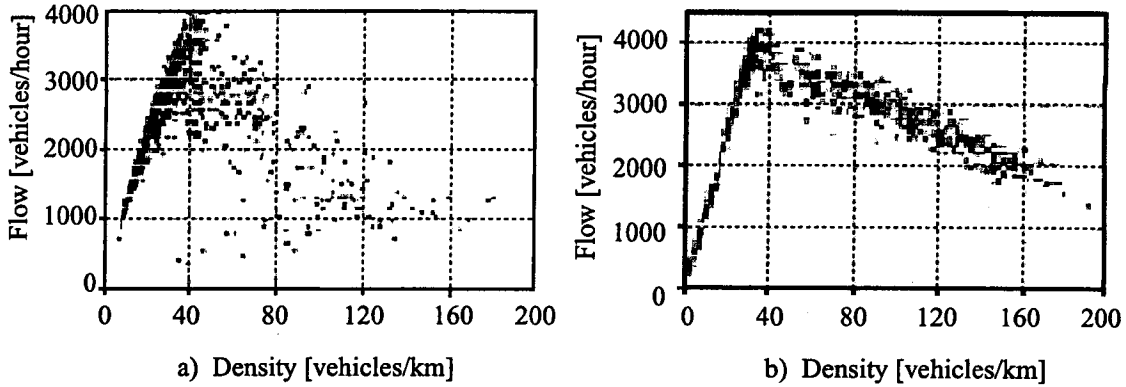


**Figure 1: Comparison of flow versus density plots for a) Field data and b) Simulation Results for a German Highway. [14]**

The Nagel-Schreckenberg model has also been used to simulate a section of a California freeway [23]. The model's results were verified by comparing the basic features of plots of flow versus speed for actual and field data. The flow versus speed diagrams showed two distinct phases, congested and uncongested flow, as well as a decline of velocity with increased flow. These comparisons were qualitative measures that showed that it is "possible to reproduce important macroscopic characteristics of traffic flow using CA models for the car-following and lane-changing behaviour." [23]

### 1.3 REPORT OUTLINE

This report provides a detailed description of the implementation of CATS, accompanied by an analysis of the model's performance when used to simulate a portion of the I-5 freeway in Seattle, Washington.

The description of the CATS model in this report follows the steps for developing traffic simulation models outlined by Ajay and Lieberman [24]. First, the input data and vehicle motion

models are described, followed by a discussion of the vehicle position update algorithm and the output statistics provided by the model.

Following the model description, a case study is presented of the I-5 freeway in Seattle, Washington. First, a congestion analysis of the field data for the proposed simulation period is presented to ensure that the model is being tested against an extensive range of traffic conditions. Second, the traffic flow simulated by the model is compared to field data by using both quantitative and qualitative measures. The conservation of cars between the model and field data and the graphs of flow versus density from the simulated and observed data are compared. Finally, these comparisons are used in an iterative manner to calibrate the input parameters for one of the vehicle motion models, and it is shown that this calibration increases the accuracy of the model.

## **2. MODEL DESCRIPTION**

The CATS model, written in C, is used to simulate multi-lane freeways. The model discretizes the roadway into homogeneous cells, which are either empty or occupied by a vehicle. At each timestep, the model applies an algorithm to update the position of each vehicle and marks the cells as empty or occupied accordingly. This section outlines the components of CATS, including a description of the steps and data needed to set up a simulation, the models for vehicle motion, the vehicle position update algorithm, and the output data provided by the model.

### **2.1 SIMULATION SETUP**

To run a simulation, the user has to provide a description of the road topology to be simulated, a description of the vehicles that are on the road, and the number of cars entering and exiting from each access and exit ramp for the duration of the simulation period.

#### **2.1.1 Road Topology**

First, the roadway to be simulated has to be defined. This definition is stored in a topology file that includes the following information:

- Length of the roadway
- Number of lanes
- HOV lane location
- Lane discontinuities (to account for the situation in which a lane ends and resumes somewhere downstream)
- Location (lane, cell) of access and exit ramps
- Location (lane, cell) of inductance loop traffic sensors on the mainlines
- Speed limit (variable)
- Cell size (feet/cell)
- Timestep duration (seconds).

These properties provide a detailed view of the roadway to be simulated and enable the user to define complicated sections of highway. The locations of access and exit ramps dictate where the vehicles will enter and exit from the roadway. (The action of the ramps can be viewed as that of a mailbox in which vehicles are periodically dropped (exit ramp) or picked up (access ramp)). The model calculates the average vehicle volume, occupancy, and speed at the location of inductance loop traffic sensors. This allows the model data to be easily compared with real-time data from the loop sensors. The legal speed limit can vary on the freeway, which is especially useful when long sections of road that pass through rural and urban areas are modeled. The cell size and timestep parameters affect the granularity of the quantization of output values such as vehicle speed and density. For example, the smaller the cell size, the finer the granularity of vehicle speed, since the vehicle speed is defined internally as cells-per-timestep.

### ***2.1.2 Vehicle Description***

The model allows for different vehicle types with the following user defined properties:

1. Vehicle length
2. Maximum acceleration
3. Maximum deceleration
4. Acceptability for travel in restricted lane type (HOV lane capability)
5. Maximum speed allowed over the legal speed limit
6. Percentage of total number of vehicles of this type.

The first five properties are used to update the vehicle positions in the roadway matrix. The vehicle length determines how many cells the vehicle will occupy; the maximum acceleration and minimum deceleration (acceleration bracket) constrain the range of motion for each vehicle in a timestep; the HOV lane capability determines whether a vehicle can move into the HOV lane; and the maximum speed allowed over the legal speed limit defines an upper bound for the vehicle speed. The percentage of total number of vehicles of this type is used to assign vehicles to the roadway from the access ramps. This property ensures a realistic distribution of car types on the roadway.

### **2.1.3 Input Data**

The CATS model runs on car volume data from the inductance loop sensors embedded in the access ramps, exit ramps, and mainline entry points (where the simulated roadway starts). The number of cars that enter and exit the roadway at these points are considered to be stochastic boundary input and output for the model. Alternatively, if these data are not available, the user can specify a probability distribution that will assign the number of cars entering and exiting the roadway at each timestep. The first option provides a more realistic simulation, but the latter option can be used when field data are not easily obtained.

One thing to note is that the embedded inductance loop sensors provide data every 20 seconds (RampTime). However, if the user wants to use a timestep of less than 20 seconds (which is often the case), the number of vehicles entering and exiting the ramps during the 20 seconds has to be distributed into each timestep. For example, if the user specifies a 1-second timestep, the model distributes the number of cars entering in 20 seconds into twenty 1-second slots. The number of cars entering or exiting a ramp at the  $i$ th timestep is  $n_i$ , StepsInRampTime is the number of timesteps in a RampTime, and  $n_1 + n_2 + \dots + n_{StepsInRampTime} = n$  is the total number of cars entering or exiting in a RampTime. The numbers  $n_i$  are assumed to be independent and identically distributed (Poisson arrivals) and are obtained with a truncated binomial distribution.

When the roadway cells are already occupied and more vehicles cannot be added, a queue of vehicles assigned to enter the roadway forms. Queued vehicles are added at the next timestep. The queue attempts to guarantee conservation in the model (i.e., to propagate the same number of vehicles in the model as in the roadway). For the off ramps, vehicles are extracted from the model in order to match the observed number of vehicles exiting the roadway. In some cases it may not be possible to extract the observed number of vehicles at the present timestep. Once again, conservation is enforced by an inverse queue that accumulates the number of vehicles to be extracted when they are available.

## **2.2 MODELS FOR VEHICLE MOTION**

The vehicle motion in CATS is governed by a set of prescribed behavioral rules that include models for the following:

- Optimal headway



- Speeding
- Breaking
- Lane changing
- Upstream effect of ramps.

These models ensure that the simulation of vehicle motion is realistic and accounts for the stochastic nature of traffic flow. All the models mentioned above have their own set of customizable input parameters and are described in the following sections.

### ***2.2.1 Model for Optimal Headway***

Space headway is defined as the “distance between successive vehicles in a traffic lane measured from some common reference point on the vehicles such as the front bumpers or front wheels.” [25] Optimal headway is the smallest safe headway a vehicle can maintain. If all vehicles maintain an optimal headway, the density of cars on the road is maximized without compromising safety factors. In CATS, optimal headway is modeled as a piecewise, linear, monotonously increasing function of the vehicle’s speed. As Figure 2 illustrates, the model is defined by the following input parameters:

- $G_0$  - value of the headway for vehicles at rest [feet]
- $\alpha_1$  - rate of increase of headway when vehicle speed is between 0 and  $S_r$  [feet/mph]
- $S_r$  - critical/ reference speed [mph]
- $\alpha_2$  - rate of increase of headway when vehicle speed is between  $S_r$  and  $S_{inf}$  [feet/mph]
- $G_{inf}$  - maximum headway [feet]

The optimal headway for any given vehicle speed ( $G(s)$ ) is calculated as follows:

$$G(s) = \begin{cases} G_0 + \alpha_1 s, & 0 \leq s \leq s_r \\ G_R + \alpha_2 (s - s_r), & s_r \leq s \end{cases} \quad (1)$$

This model captures the fact that the linear variation of the safe headway increases more rapidly for small headways than for larger headways. At each timestep, this model determines the optimal headway for the vehicle, given its speed. This information is used to determine the motion goal of the vehicle, as explained in a following section.

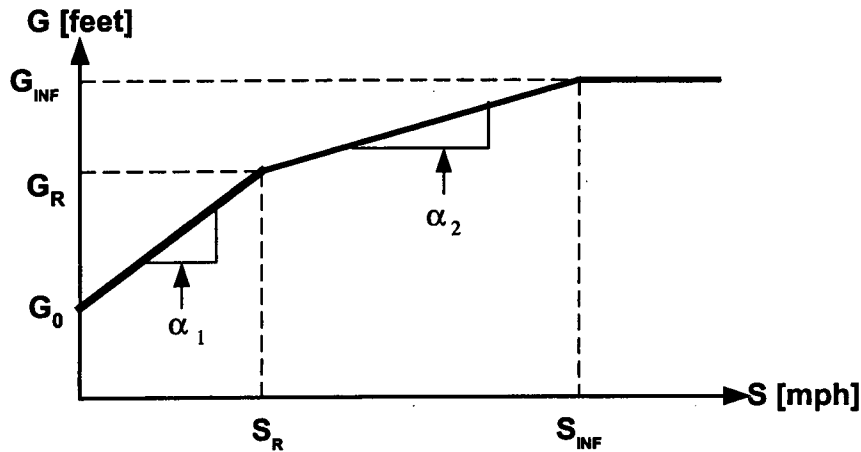


Figure 2: Piecewise linear model for optimal headway.

### 2.2.2 Model for Speeding

The model describes the fact that some drivers do not always adhere to the legal speed limit ( $s_L$ ), and therefore, a non-negligible fraction of vehicles do speed. In CATS, the probability that a vehicle will speed is governed by the  $P_{speeding}$  parameter, and the behaviour of these vehicles is defined by a probabilistic set of rules that depend on the following speed dependent probabilities:

- $P_{keep}$  - Probability of maintaining speed
- $P_{acc}$  - Probability of increasing speed/accelerating
- $P_{break}$  - Probability of decreasing speed/decelerating

subject to the following conditions:

$$\begin{aligned}
P_{keep}(s) + P_{acc}(s) + P_{break}(s) &= 1 \\
P_{break}(s_L) = P_{acc}(s_{max}) &= 0
\end{aligned} \tag{2}$$

where  $s_{max} = s_L + \Delta s$  is the maximum user-assigned speed for this type of vehicle. As illustrated in Figure 3, as the vehicle speed increases,  $P_{keep}$  and  $P_{acc}$  decrease toward 0.0, and  $P_{break}$  increases toward 1.0.

A random number  $\xi \in [0,1]$  is used to decide whether the vehicle will decelerate to the legal speed, remain at the same speed, or accelerate to the maximum speed. The following set of rules are applied at each timestep.

$$\begin{aligned}
\xi \leq P_{keep} &\rightarrow s' = s \text{ (maintain speed)} \\
P_{keep} \leq \xi \leq P_{keep} + P_{break} &\rightarrow s' = s_L \text{ (break)} \\
\text{else} &\rightarrow s' = s_{max} \text{ (accelerate)}
\end{aligned} \tag{3}$$

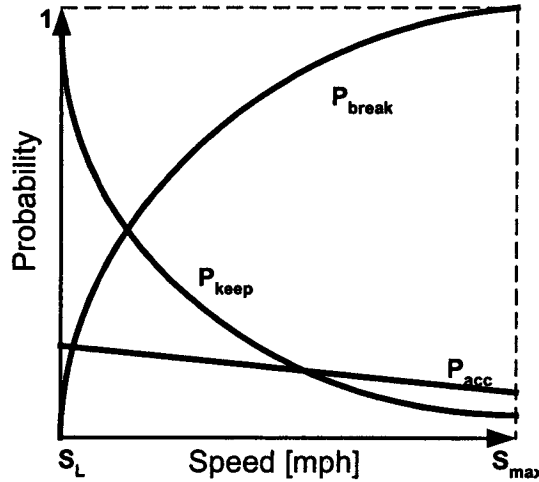


Figure 3: Shape of probability functions in the speeding model.

### 2.2.3 Model for Breaking

The motivation for this model is that drivers who are driving with unsafe headways may choose to break spontaneously when they get too close to the car ahead. CATS accounts for this

phenomenon by introducing  $P_{break}$ , the probability of breaking when the headway is unsafe and the vehicle is not speeding. The probability is used to determine whether vehicles with unsafe headways will break to achieve an optimal headway or accelerate to reach a desired speed. This is implemented as follows:

$$\text{With random } \xi \in [0,1]: \begin{cases} \xi \leq P_{break} & \rightarrow \text{goal is optimal headway} \\ \text{Else} & \rightarrow \text{goal is desired speed} \end{cases} \quad (4)$$

### 2.2.4 Model for Lane Changing

The model for lane changing in CATS depends on several factors that include local road topology (HOV lanes, proximity of access and exit ramps downstream), local vehicle density, and vehicle distribution. The model includes both a deterministic and random component.

The deterministic component of the lane changing model is based on the assumption that a vehicle will change lanes if the traffic conditions are better on either of the neighboring lanes (i.e., drivers of vehicles attempt to travel at the maximum allowed speed within safety margins).

The safety function, which is defined as the difference between the actual and optimal headway of the vehicle, assuming that the vehicle will move into an adjoining lane, is compared with the safety function, assuming the vehicle stays in its present lane, and the most favourable value is used to select the new lane of travel.

The safety function for the present lane is defined as the difference between the vehicle's actual headway and optimal safe headway for the current speed. Figure 4 presents the motion of two vehicles ( $V_A$  and  $V_B$ ) in one lane during a timestep. The safety function  $Z_A$  of vehicle  $V_A$  at time  $t + \Delta t$  is as follows:

$$Z_A(t + \Delta t) = \begin{cases} G_A(t) + \Delta x_B - \Delta x_A - G_A(s(t + \Delta t)) = G_A(t + \Delta t) - G_A(s(t + \Delta t)), & \Delta x_A < G(t) + \Delta x_B \\ -\infty & , \text{else} \end{cases} \quad (5)$$

where  $G_A(t)$  is the headway at time  $t$  between vehicle  $A(V_A)$  and vehicle  $B(V_B)$ ,  $\Delta x_A$  and  $\Delta x_B$  are the distances traveled in time  $\Delta t$  by  $V_A$  and  $V_B$ , and  $G_A(s(t + \Delta t))$  is the optimal headway corresponding to the speed of vehicle  $V_A$  at time  $t + \Delta t$ . Note that this calculation is only valid when  $\Delta x_A < G(t) + \Delta x_B$ . This corresponds to the assumption that vehicle  $A$  will not overtake vehicle  $B$  in the timestep.

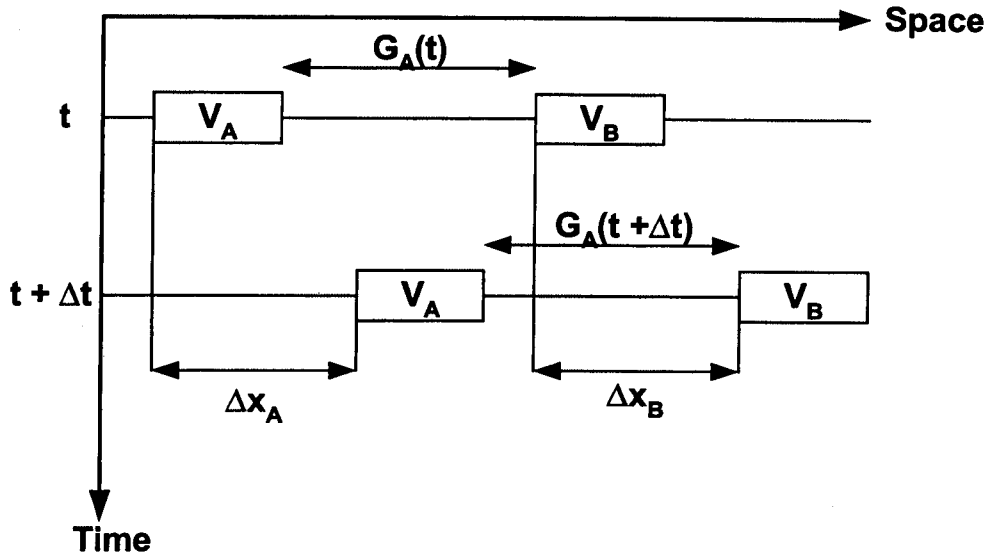


Figure 4: Update of vehicles in same lane.

The safety function for the adjoining lane depends on the vehicles that will be ahead and behind the vehicle if it changes lanes. Figure 5 illustrates vehicle  $V_A$  in lane 2 moving to lane 1 in front of vehicle  $V_C$  and behind vehicle  $V_D$ . To determine the safety function for vehicle  $V_A$  if it moves to lane 1, the safety functions at time  $t + \Delta t$  for both vehicle  $V_C$  and vehicle  $V_A$  need to be considered. The equations are as follows:

$$\begin{aligned} Z'_A(t + \Delta t) &= G_A(t + \Delta t) - G_A(s(t + \Delta t)) \\ Z'_C(t + \Delta t) &= G_C(t + \Delta t) - G_C(s(t + \Delta t)) \end{aligned} \quad (6)$$

Combining  $Z'_A(t + \Delta t)$  and  $Z'_C(t + \Delta t)$ , the safety function for vehicle  $V_A$  if it moves to lane 1,  $Z^1_A(t + \Delta t)$ , is given by the following:

$$Z^1_A(t + \Delta t) = \max[Z'_A(t + \Delta t), (Z^1_A(t + \Delta t) + Z'_C(t + \Delta t)) / 2] . \quad (7)$$

The safety function for  $Z^3_A(t + \Delta t)$ , which assumes vehicle  $V_A$  moves into lane 3 instead of lane 1, can be computed in the same way. Finally, the following safety functions are compared:

- $Z^1_A(t + \Delta t)$ , the safety function of vehicle  $V_A$  if it moves to lane 1,
- $Z^3_A(t + \Delta t)$ , the safety function of vehicle  $V_A$  if it moves to lane 3,

- $Z_A(t + \Delta t)$ , the safety function of vehicle  $V_A$  if it does not change lanes,

and a decision is made as to whether the vehicle should change lanes, depending on the following rules:

$$\begin{aligned}
 Z_A(t + \Delta t) \geq 0 &\rightarrow \text{stay in current lane} \\
 Z_A(t + \Delta t) < 0 &\rightarrow \begin{cases} Z_A(t + \Delta t) \geq \max(Z_A^N(t + \Delta t)) &\rightarrow \text{stay in current lane} \\ Z_A(t + \Delta t) < \max(Z_A^N(t + \Delta t)) &\rightarrow \text{change to lane } N \end{cases}
 \end{aligned} \tag{8}$$

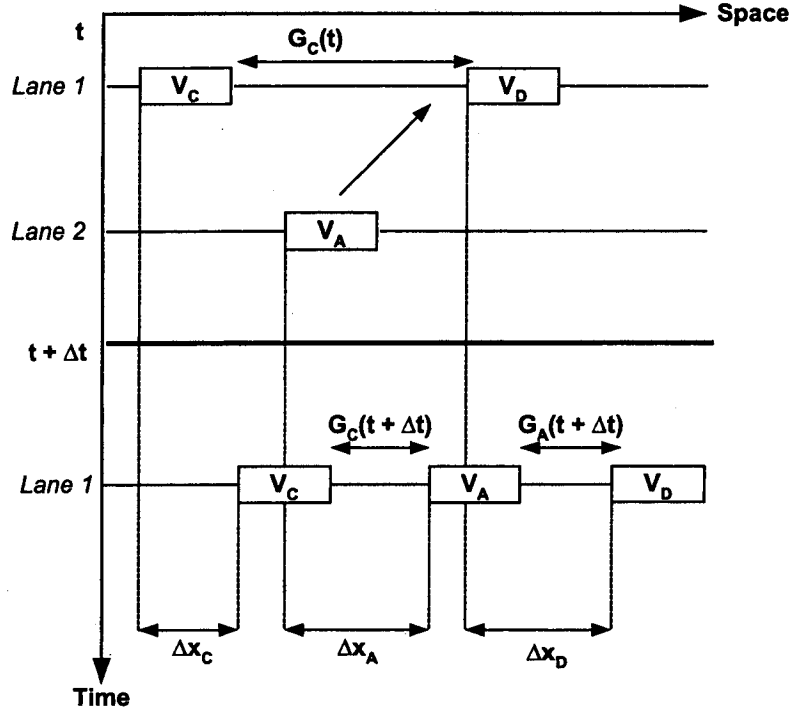


Figure 5: Update of vehicles when changing lanes.

Note, if one of the neighboring lanes does not exist, the corresponding safety function is assumed to be  $-\infty$ . The decision rules outlined in (8) imply that the vehicle should not make a lane change unless the safety conditions are better in an adjoining lane. However, in order to introduce a degree of randomness into the vehicle motion, there are times when these rules are not followed. This is implemented by the random component of the lane changing model, which includes the following probabilities:

- $P_{stay}$  – Probability that vehicle will remain in the same lane regardless of the traffic conditions in other lanes.
- $P_{change}$  – Probability that vehicle will change lanes even though traffic conditions in its original lane satisfies its speed and safety goals. If there are two neighboring lanes, the probabilities  $P_{left}$  and  $P_{right}$  are used to determine the direction of lane change.

In summary, the basic assumption underlying this model is that a driver will want to travel in the lane with the most favourable traffic conditions, but in a small number of cases, the driver will either change lanes or stay in a lane regardless of the existing conditions.

### ***2.2.5 Model for Upstream Effect of Ramps***

This model is an extension of the lane changing model; it considers the effect of access and exit ramps on lane changing probabilities. CATS considers ramps to be stochastic boundary conditions. The user defines the length of roadway before a ramp and the number of lanes in the roadway that will be affected by the access and exit ramps. In addition, a weight coefficient can be specified for the ramps. Over this segment of roadway, the probabilities  $P_{left}$  and  $P_{right}$  specified in the random component of the lane changing model are multiplied by the ramp weight coefficient to increase the probability that vehicles will move toward an exit ramp or away from an access ramp. Also, the probability of vehicles moving out of the exit lane when an exit ramp is close by is decreased so that vehicles have a chance to exit.

### **2.3 ALGORITHM FOR UPDATING VEHICLE POSITION**

The CATS model sequentially updates vehicle positions, beginning with the vehicles nearest the downstream end of the model and proceeding in a counterflow direction until the beginning of the roadway is reached. The side of the roadway with which to start updating (e.g., inside or outside lane) is selected randomly to minimize biasing of the results, and the update proceeds across any lanes defined in the model.

The algorithm used to update the position of each vehicle considers all the vehicle motion models described above. The main idea behind this algorithm is to determine the goal of the vehicle's motion, which can be to establish either an optimal headway or a desired speed, in the

timestep and then calculate the acceleration needed for the vehicle to meet its motion goal. The following sections explain the steps of the algorithm. This is accompanied by a high-level block diagram of the algorithm, as shown in Figure 6, and a detailed view of the implementation of the algorithm, as shown in Figure 7 a,b,c. Note that all the  $\xi_n$  are random numbers  $\in [0,1]$ . These numbers are used to introduce a degree of stochasticity into the model.

### ***2.3.1 Determine Vehicle Motion Goal***

First, the vehicle's position and speed are determined. Then the headway between the vehicle and the one ahead is calculated and compared with the optimal headway for a vehicle going at this speed, as described in the optimal headway model. If the headway is unsafe (i.e., less than the optimal value) and the model for breaking can be applied ( $\xi_1 < P_{break}$ ), the goal of vehicle motion for this timestep is to establish an optimal headway behind the vehicle ahead. If the actual headway is safe (i.e., greater than or equal to the optimal one), the goal of motion for the vehicle is to reach a desired speed.

### ***2.3.2 Optimal Headway Goal***

If the motion goal of the vehicle is to have an optimal safe headway, the acceleration needed to move the vehicle into the desired position is calculated. Note that the value of acceleration is constrained by the acceleration bracket specified in the vehicle description, and if the acceleration needed exceeds the maximum acceleration possible, the vehicle will accelerate at its maximum acceleration. Finally, the vehicle's speed and position are updated and the algorithm iterates on the next vehicle in the roadway.



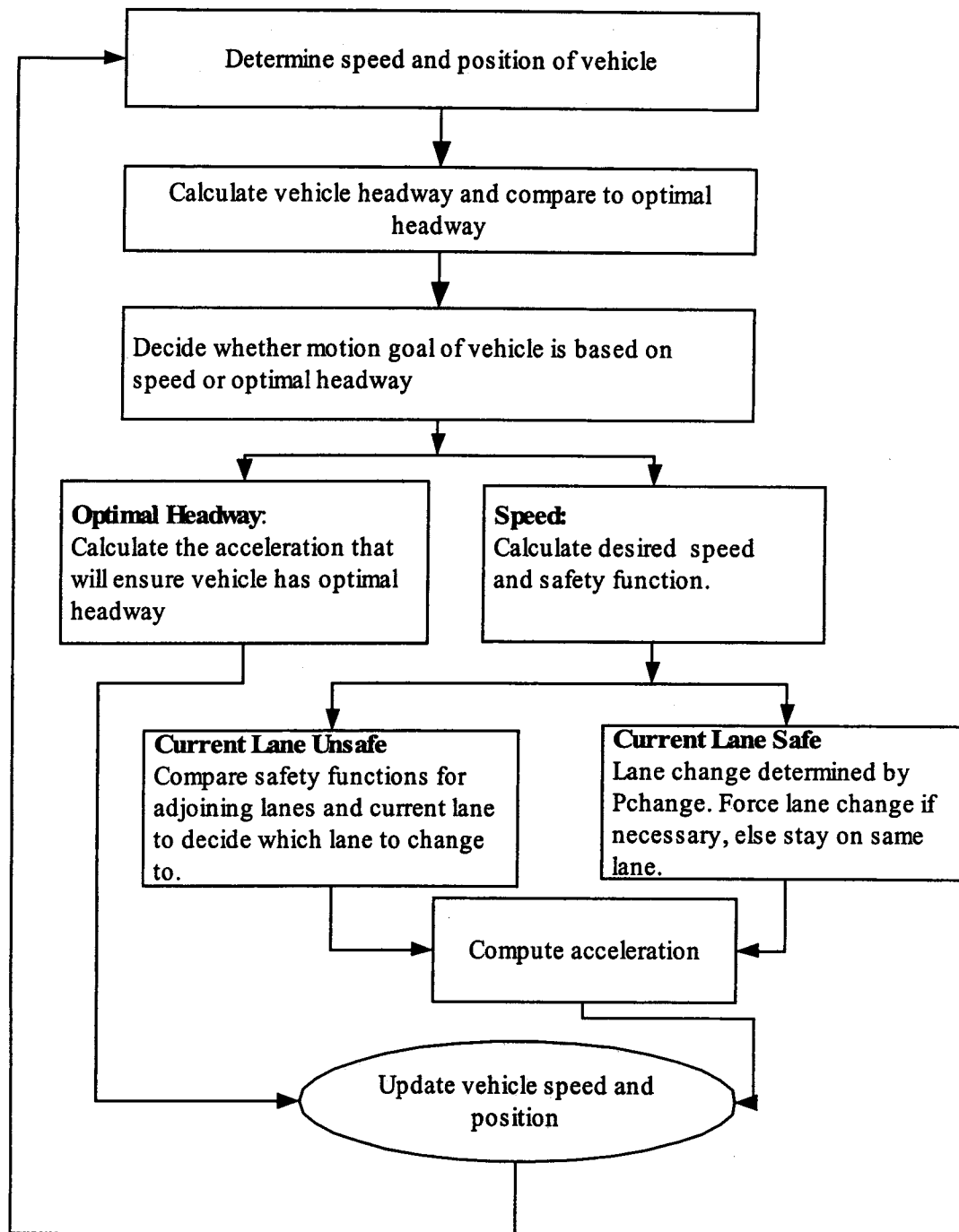


Figure 6: Block diagram for CATS vehicle update algorithm.

### **2.3.3 Desired Speed Goal**

If the motion goal of the vehicle is to reach a desired speed, the algorithm illustrated in Figure 7 b and c is executed. This includes the models for speeding, lane changing, and upstream effect of ramps, as described in the previous section.

First, if the vehicle is not speeding ( $s \leq s_L$ ), it will either accelerate to the legal speed limit or maximum vehicle speed ( $s_{max}$ ), depending on the  $P_{speeding}$  probability. If the vehicle is already above the speed limit, the model for speeding will be applied to determine the vehicle's desired new speed. Given the desired speed of the vehicle, the acceleration needed to meet this goal and the new position of the vehicle is calculated.

Second, the safety function assuming the vehicle will not change lanes is calculated. If staying in the same lane is a safe option, the vehicle will do so unless the random component for the lane changing model ( $P_{change}$ ) comes into effect, whereby the vehicle will change lanes regardless of the traffic conditions. Otherwise, if it is unsafe to stay in the same lane, the safety function for the adjoining lanes is computed, and the vehicle will change lanes into the adjoining lane with the best safety function. Once a decision has been made as to whether the vehicle will change lanes, the acceleration is recomputed, and the vehicle's speed and position are updated appropriately. Note that if the acceleration needed to meet the vehicle's motion goal will result in unsafe motion, the acceleration is decreased to ensure safe propagation of vehicles.

## **2.4 OUTPUT DATA**

Traffic stream parameters can be classified by the same categories as traffic simulation models: "macroscopic parameters characterize the traffic stream as a whole and microscopic parameters characterize the behaviour of the traffic stream with respect to each other." [25] Volume, speed, and density are examples of macroscopic parameters, while headway is a microscopic parameter [25].

The CATS model accumulates the average volume, occupancy, and vehicle speed at each time step from the locations designated by the user in the input road topology file. The model also records the number of vehicles entering and exiting the roadway, changing lanes, speeding, and braking at each timestep.

In addition, the time needed to run the simulation is computed so that the efficiency of the model can be measured.

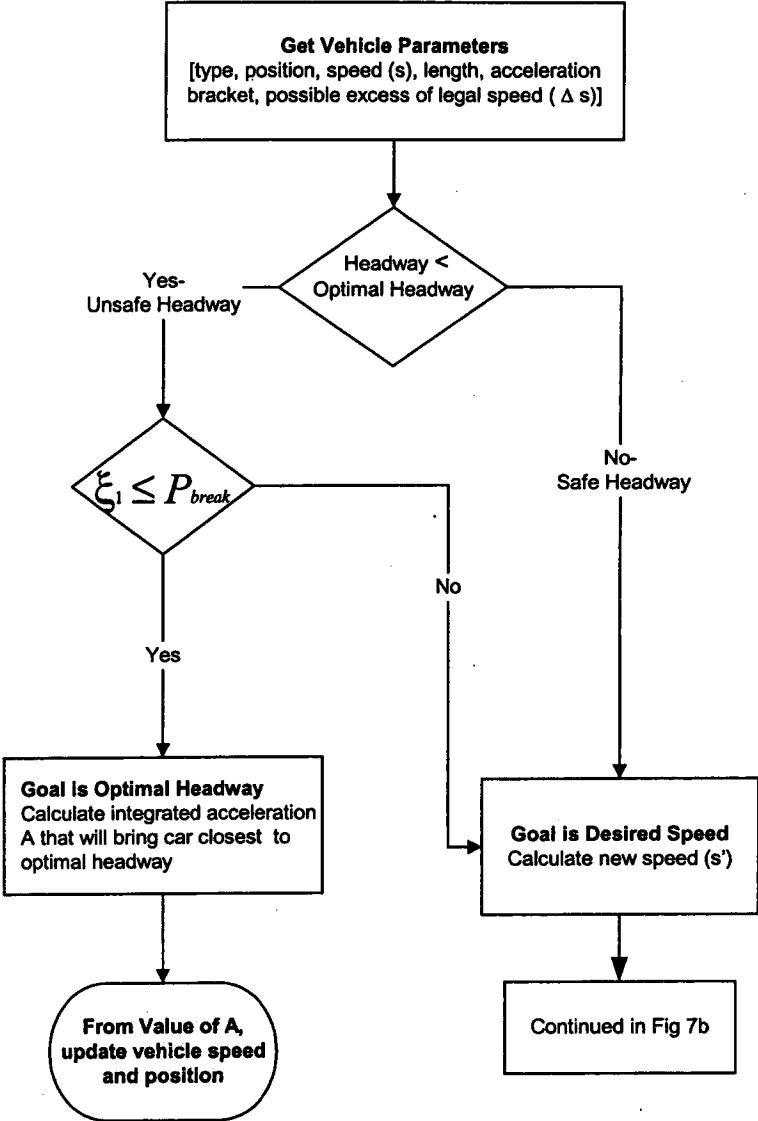
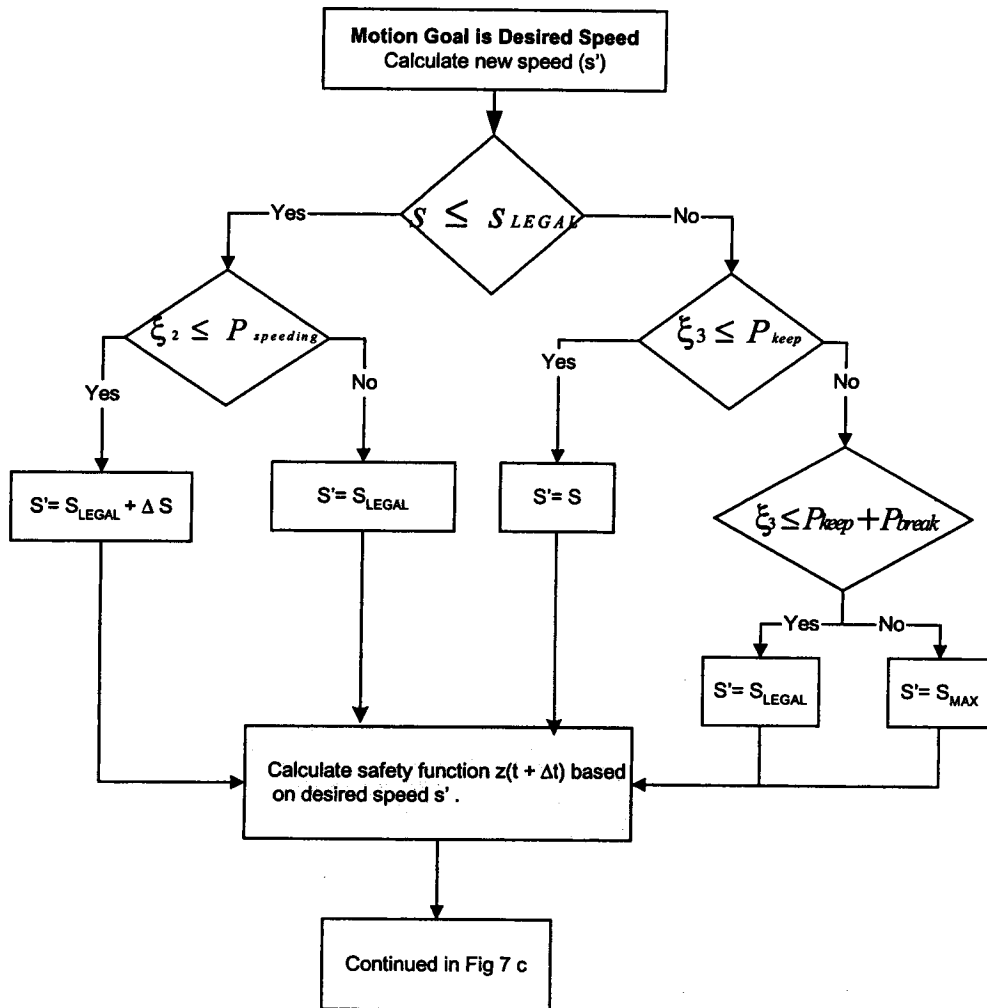
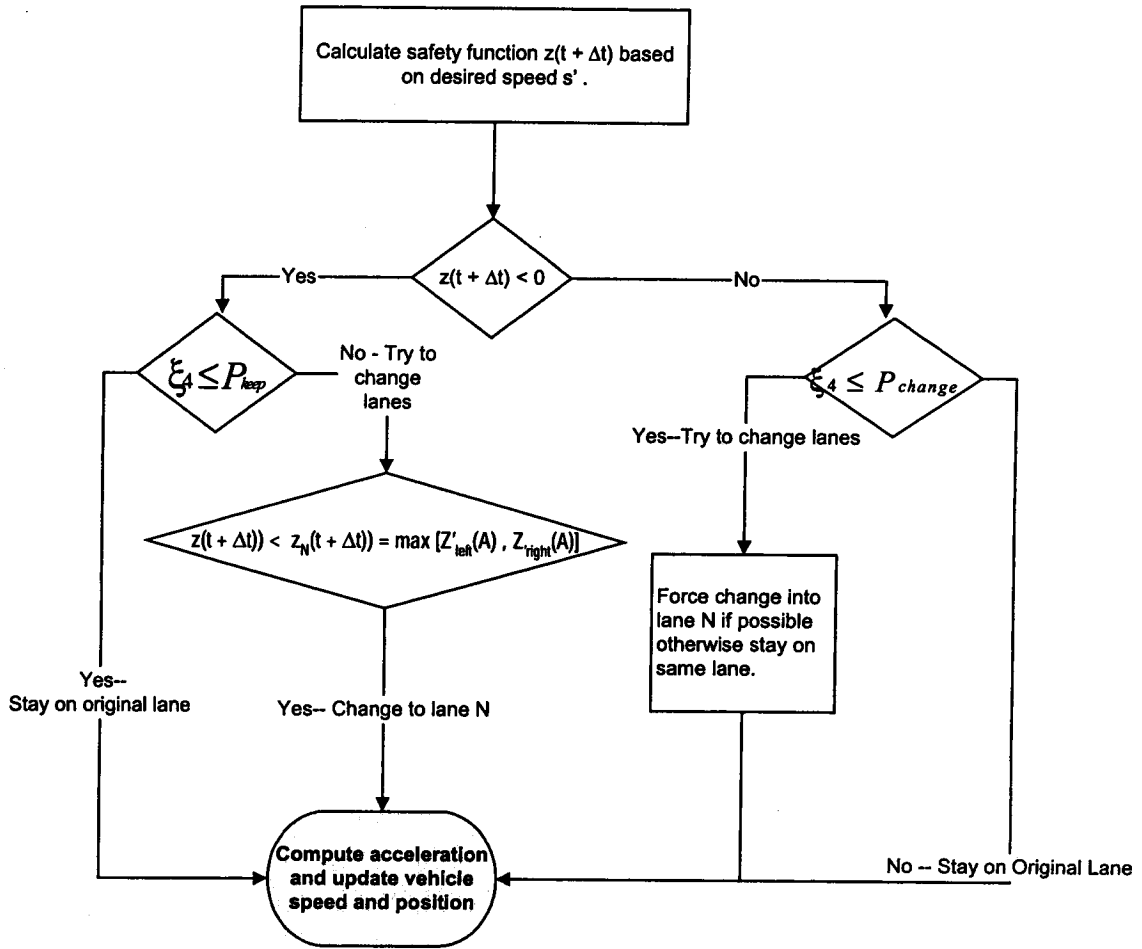


Figure 7: Flow chart for vehicle update algorithm.

(a) Determine the goal of vehicle motion.



**Figure 7 (continued): Flow chart for vehicle update algorithm.**  
**(b) Determine desired speed.**



**Figure 7 (continued): Flow chart for vehicle update algorithm.**  
**(c) Apply lane changing model to update vehicle position.**

### **3. CASE STUDY**

To evaluate the performance of the CATS model, a case study was conducted on the southbound traffic of the I-5 freeway in Seattle, Washington. The following sections describe the setup of the simulation, the analysis of the field data, the methods used to compare the model's results to field data, and the steps taken to optimize the performance of the model.

#### **3.1 SIMULATION SETUP**

In order to set up a simulation, the following must be defined: the roadway topology, vehicle description, simulation period, and input data source.

##### **3.1.1 Road Topology**

The section of I-5 used in this analysis is in North Seattle between the 228th Street SW and E Galer Street intersections, as shown in the map of Figure 8. This section is approximately 1.1 miles long and has between three and five lanes of traffic in each direction. The leftmost lane is designated the HOV lane, and there are 20 access ramps, 13 exit ramps, and 108 inductance loop sensors on the mainlines. The model was run with a cell length of 8 feet and a timestep of 1 second. The posted speed limit on the roadway is 60 miles per hour for the entire section. The percentage of speeding vehicles was determined by calculating the speed values from the data from the embedded loop sensors in the roadway. Figure 9 shows a histogram of the percentage of vehicles speeding over all the traffic sensors on the section of road that was simulated. This histogram shows that the mean value of the percentage of speeding vehicles was 20.6.

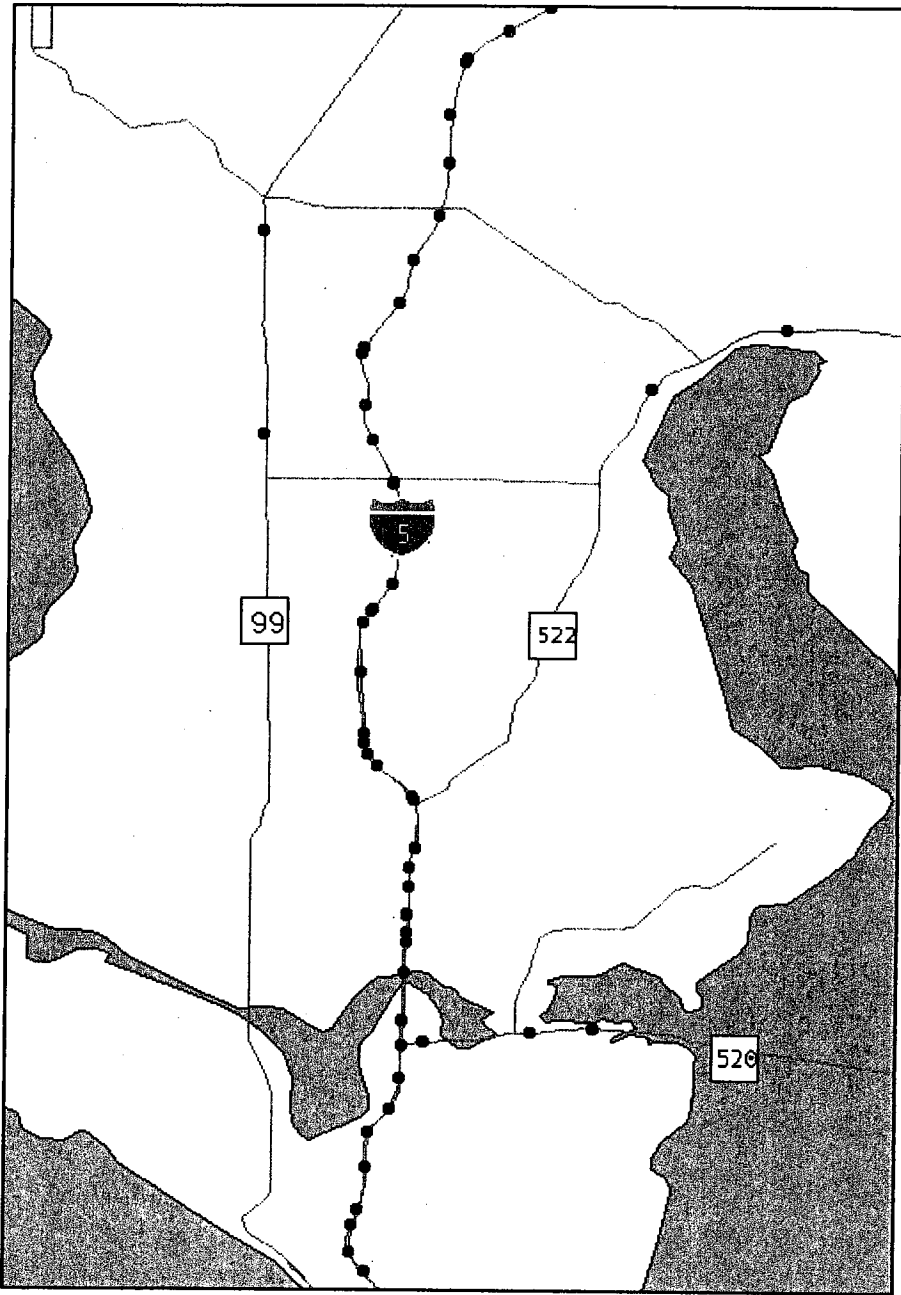


**Figure 8: I-5 freeway section used in case study.**

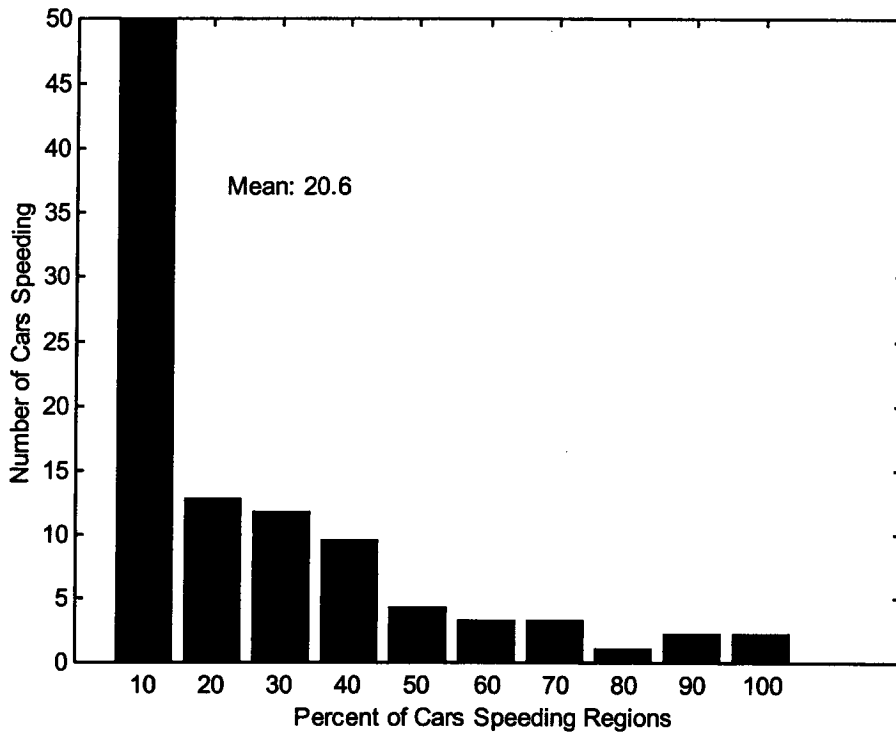


**Figure 9: Percentage of speeding vehicles on the roadway.**

### ***3.1.2 Vehicle Description***

Three types of vehicles were defined for the roadway:

1. Passenger cars that travel on general purpose or HOV lanes
2. Passenger cars that travel on general purpose lanes only
3. Trucks that travel general purpose lanes only.

The passenger cars were 20 feet long and the trucks were 40 feet long, and the distribution of these vehicles on the road was 12 percent, 82 percent, and 6 percent respectively. These values are consistent with the definitions published by the American Association of State Highway and Transportation Officials (AAHSTO) [25].



### ***3.1.3 Simulation Time Period***

The model is initially empty and fills as vehicles propagate downstream. The initial state of the model will have a significant effect on the downstream predictions. Thus, the initial state must match the steady state behavior of traffic in the roadway. To meet this need, the model simulates the traffic over a training period to eliminate transient effects. In our case, the training period used was the nine hours from midnight to 9:00 am, which allowed for approximately 49 traversals of the model, given an 11-mile section where traffic was flowing at approximately 60 mph; one traversal of the model took 11 minutes. This was sufficient to establish a steady state behavior. Following this, the model simulated traffic for a testing period of twelve hours from 9:00 am to 9:00 pm, and the state of the system at the end of the training period was used as the initial state. The traffic measurements calculated by the model for this time period were compared to field data for the same period.

### ***3.1.4 Input Data from Roadway***

Volume data from embedded inductance loop sensors on the access and exit ramps on I-5 provided boundary input and output conditions for the model, and data from inductance loop sensors on the mainlines were used to compare the model predictions to observed traffic. The black dots on the map in Figure 8 indicate the locations of embedded traffic sensors on the highway. Traffic sensors are 6-foot square loops of copper wire connected to cabinets located along the highway. Electronic devices are used to measure changes in inductance in the loop and calculate the aggregate number of vehicles that drive over the loop (volume) and the average percentage of time a vehicle occupies the road (occupancy) during a sampling interval. These volume and occupancy data are sampled every 20 seconds, 24 hours a day, and sent to the Traffic Systems Management Center (TSMC) at the Washington Department of Transportation (WSDOT).

## **3.2 ANALYSIS OF FIELD DATA**

Before the field data were used to run the simulation, they needed to be analyzed to ensure that they were valid, complete, and covered an acceptable range of traffic conditions. This was done with the daily traffic count analysis and level of service analysis described in the following sections.

### **3.2.1 Traffic Count Analysis**

To ensure that the data from the inductance loop sensors were complete, the number of 20-second data samples ( $n$ ) available from all the sensors in the proposed simulation period was counted. For example, for a 12-hour simulation period, there should be  $12 \text{ hours} * 60 \text{ minutes/hour} * 3 \text{ samples/minute} = 2160$  data samples. The data completeness measure was defined as  $n/2160$ . The data samples also contained a flag that indicated whether the data were valid. Data were marked invalid if a sensor was malfunctioning. The count quality measure was defined to be  $v/2160$ , where  $v$  is the number of valid data samples. Finally, the sensor validity was defined to be  $v/n$ . For the proposed simulation period, the data completeness, count quality and sensor validity measures were tabulated to ensure the data set used as input to the model was complete and valid.

### **3.2.2 Level of Service Analysis**

An effective traffic model needs to accurately simulate traffic flow through a wide range of traffic conditions, from very light traffic to complete congestion. To ensure that the traffic in the proposed simulation period used in this case study satisfied these requirements, a level of service analysis was done on the volume data taken from the embedded loop traffic sensors.

Level of service is a qualitative measure, defined in the Highway Capacity Manual, that “describes operational conditions within a traffic stream and their perception by motorists and passengers. A level of service definition generally describes these conditions in terms of such factors as speed and travel time, freedom to maneuver, traffic interruptions, comfort and convenience, and safety.” [26] Using the letters A-F, six levels of service are defined. Level of service A, the best level of service, represents a free-flow condition in which vehicles are easily maneuvered within the traffic stream. Level B represents reasonably free-flow conditions in which vehicle motion is slightly restricted. Level C describes stable flow, but at this level, small increases in flow will cause substantial traffic congestion. Level D borders on unstable flow, where even minor accidents can create substantial queues. Level E describes operations at capacity. At this level, there are virtually no usable gaps in the traffic stream, and any incident will produce a serious breakdown with extensive queuing. Level F, the worst level of service, represents a breakdown of traffic flow in which the rate of vehicle arrival exceeds the capacity of the roadway [26]. “For each type of facility, levels of service are defined based on one or more operational

parameters which best describe operating quality for the subject facility type. The parameters selected to define levels of service for each facility type are called ‘measures of effectiveness’ (MOE).” [26] A MOE “describes traffic operations in terms discernible by motorists and their passengers.” [25] For an uninterrupted flow facility such as a freeway, the MOEs used to describe levels of service are density ( $D$ ) and flow rate/volume ( $v$ ). Density, measured in vehicles/mile/lane, “describes the proximity of other vehicles in the traffic stream. It is a surrogate measure for driver comfort and ease, and for the ability to maneuver within the traffic stream.” [25] The flow rate or volume, measured in vehicles/hour/lane, “is the maximum hourly rate at which vehicles can reasonably be expected to traverse a point or uniform section of a lane or roadway during a given time period under prevailing roadway, traffic and control conditions while maintaining a designated level of service.” [26] Table 1 quantifies the levels of service for freeway sections described above using density, flow rate, and speed measures [26].

**Table 1: Levels of service definition for freeway sections.**

<b>Level of Service</b>	<b>Density (vehicles/mile/lane)</b>	<b>Flow/Volume (vehicles/hour/lane)</b>	<b>Average Speed (miles/hour)</b>
A	≤ 12	≤ 700	60
B	≤ 20	≤ 1100	57
C	≤ 30	≤ 1550	54
D	≤ 42	≤ 1850	46
E	≤ 67	≤ 2000	30
F	> 67	Highly variable, unstable	No movement

The histogram Figure 10 shows the percentage of total volume data samples from the inductance loop sensors in each level of service (LOS) region for lanes 1 through 4 on the roadway for the period that was simulated. The level of service region boundaries were determined with the data from Table 1. The lane numbering goes from right to left. These plots show that all levels of service were represented in the simulation period. It is interesting to note that the different lanes had different LOS distributions. Lane 1, the rightmost lane, which contained the access and exit ramps, was the least congested (i.e., had the highest LOS A percentage). The low congestion in this lane may be attributed to the fact that most vehicles did not stay in this lane for long periods of time, preferring to move to the uninterrupted lanes to the left until they needed to exit the freeway.

Lane 4, the leftmost lane, had the highest level of congestion. This lane experienced an LOS of D or above for 25 percent of the simulation period. This is also interesting because it indicates that the designated “fast lane” may in fact have had the highest level of congestion. In summary, the LOS analysis of the volume data from the field indicated that all levels of congestion from light traffic to breakdown flow were represented in the proposed simulation period of 9:00 am to 9:00 pm.

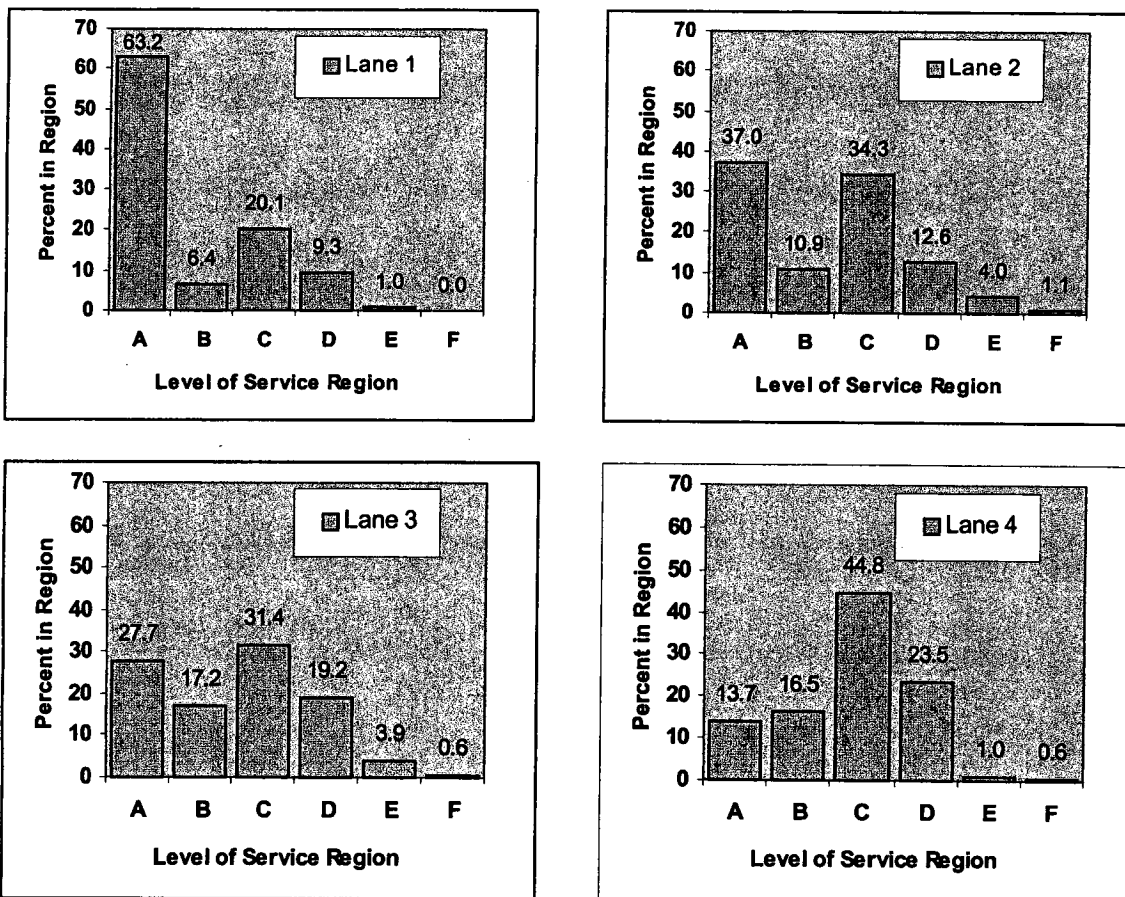


**Figure 10: Level of service distribution by lane using volume data from sensors in the roadway.**

### 3.3 METHODS OF COMPARISON

To make comparisons between the simulated data and field data, the percentage difference between the total number of cars on the actual and simulated roadway was calculated, and the plots of traffic flow versus density generated by the actual and model data were compared.

#### 3.3.1 Conservation of Cars

Conservation of cars is a quantitative metric that is defined as the percentage difference in the average number of cars in the model and the roadway for the simulation period. The metric is defined as follows:

$$Q = \frac{1}{N} \sum_{i=1}^n \frac{(\bar{V}_i^{MODEL} - \bar{V}_i^{ACTUAL})}{\bar{V}_i^{ACTUAL}} \times 100, \quad (9)$$

where  $\bar{V}_i^{MODEL}$  is the mean volume at a loop location calculated by the CATS model,  $\bar{V}_i^{ACTUAL}$  is the mean volume given by the embedded inductance loop traffic sensor on the roadway at the same location, and  $N$  is the number of loop locations defined in the roadway to be simulated.  $\bar{V}_i^{ACTUAL}$  is calculated by taking the the sample mean of the volume given by the  $i$ th loop traffic sensor at each time step, and  $\bar{V}_i^{MODEL}$  is calculated by taking the sample mean of the volume output by the model at the same location as the loop sensor.  $T$  is the total number of 20-second timesteps in the simulation period.

$$\begin{aligned} \bar{V}_i^{MODEL} &= \frac{1}{T} \sum_{j=1}^T V_{ij}^M \\ \bar{V}_i^{ACTUAL} &= \frac{1}{T} \sum_{j=1}^T V_{ij}^A \end{aligned} \quad (10)$$

This metric is a good measure of the model's performance because it measures how accurately the model can match the boundary input and output conditions imposed by the access and exit ramp volume data. A positive value of  $Q$  indicates that more cars than needed are in the simulated roadway, and similarly, a negative  $Q$  value indicates that the simulated roadway does not have enough cars.

### 3.3.2 Traffic Flow versus Density Plots

The traffic flow/volume [vehicles/hour/lane] versus density [vehicles/mile/lane] plot, often referred to as the fundamental diagram, is one of the most basic measurements in traffic engineering [23]. It represents a relationship between the three macroscopic variables: average speed  $S$  (miles/hour), flow  $v$  (vehicles/hour/lane), and density  $D$  (vehicles/mile/lane). These variables are related by the following equation [26]:

$$v = S \times D \quad (11)$$

Figure 11 shows a graphical relationship between traffic flow and density, as illustrated in the Highway Capacity Manual [26]. This plot shows that flow is 0.0 for two different conditions:

1. When no cars are on the road (density is 0.0)
2. When the density becomes so high that vehicles cannot move. This density is referred to as the jam density,  $D_j$ .

The maximum flow value is called the roadway capacity. The density value corresponding to this flow value is referred to as critical density,  $D_c$ . When density is greater than  $D_c$ , the roadway can no longer support the increase in cars, and flow deteriorates toward 0.0. As shown in Figure 11, LOS A-E reside on the left-hand stable flow region of the flow versus density plot, and LOS F covers the forced flow region on the right-hand side. The shape of the flow density curve is derived from the linear speed-density model proposed by Greenshields in 1934 [26, 27, 28] as a result of field studies conducted in Ohio,

$$S = S_f \left( 1 - \frac{D}{D_j} \right) \quad (12)$$

where:  $D$  = Density [vehicles/mile/lane]

$D_j$  = jam density

$S_f$  = free flow speed, the theoretical speed of traffic when density is zero.

To find the corresponding model for flow ( $v$ ) versus density ( $D$ ), the relationship  $v = S \times D$  can be used. Substituting  $S = v/D$  into the equation

$$\frac{v}{D} = S_f - \frac{S_f}{D_j} D \quad , \quad (13)$$

and then solving for  $v$ , yields

$$v = S_f D - \frac{S_f}{D_j} D^2 \quad . \quad (14)$$

As shown in equation (13), a linear speed density model results in a second order polynomial or parabolic flow-density relationship consistent with the theoretical relationship illustrated in Figure 11 [25].

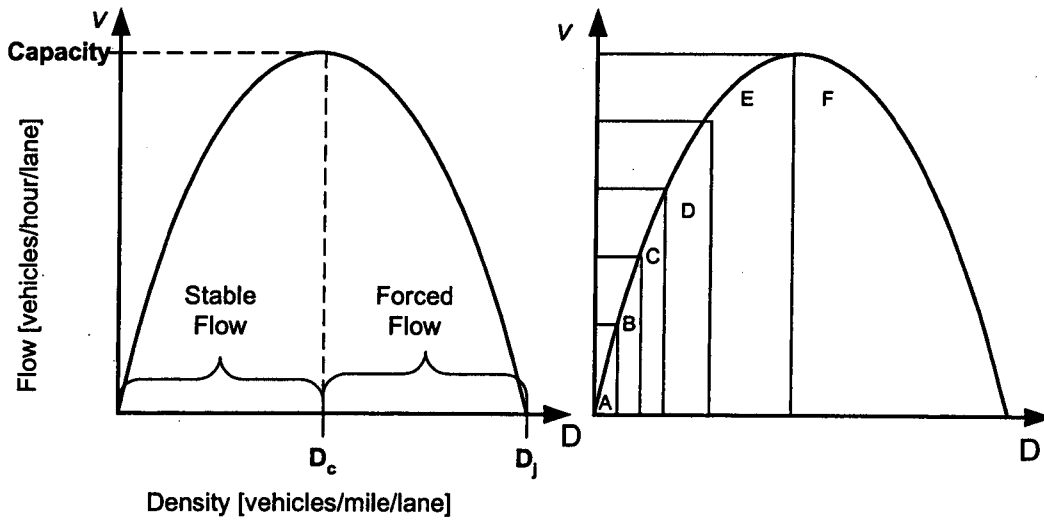


**Figure 11: Theoretical relationship between traffic flow and density and illustration of levels of service.**

As mentioned earlier, the results of the other models discussed in the existing literature are often validated by comparing the plot of traffic flow and density generated by the simulated results and field data. The trend in the literature is to limit this comparison to a qualitative one in which the general characteristics of the plots are visually compared and discussed [10, 14, 23]. In this work, the flow versus density plots were compared both qualitatively and quantitatively, as described in the following section.

### 3.4 PERFORMANCE OF THE CATS MODEL

The performance goal of the CATS traffic simulation model is to accurately reproduce traffic flow on the road at user-specified locations. The volume data from the access and exit ramps on the roadway serve as boundary vehicle input and output conditions, and the models for vehicle motion are applied to propagate the vehicles correctly at each timestep. Modifying the input parameters of these vehicle motion models can optimize the performance of CATS.

#### 3.4.1 System Model

Figure 12 illustrates a system model for the CATS model and the roadway operating in parallel. This idealizes the CATS model and the roadway as black boxes with inputs and outputs. The input to the roadway is  $\bar{X}$ , the volume data from the embedded inductance loop sensors on the access and exit ramps. The input to CATS is  $\bar{X}$ , the volume data from the access and exit ramps on the roadway and  $\theta$ , the input parameters on which the vehicle motion models are based.  $H_M$  and  $H_R$  are the system functions for the CATS model and roadway, respectively. Note that  $H_M$  is a function of  $\theta$ . The output from the roadway is  $\bar{Y} = H_R \bar{X}$ , the volume data from the traffic sensors at downstream locations, and  $\hat{Y} = H_M(\theta) \bar{X}$  is the calculated output from the model at the same locations. The accuracy of CATS is determined by comparing  $\bar{Y}$  and  $\hat{Y}$ . However, as shown in the system, this means that  $H_R$  and  $H_M(\theta)$  should match. This is attempted by calibrating  $\theta$ , the input parameters for the vehicle motion models.

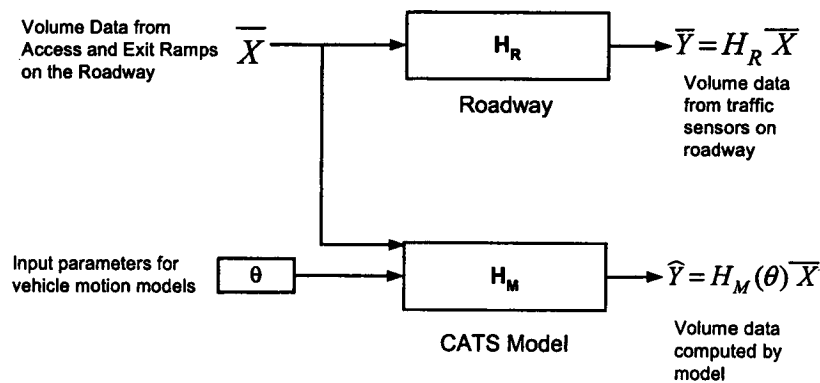


Figure 12: System model for CATS and roadway.



### 3.4.2 Calibration of Model for Optimal Headway

An examination of the vehicle position update algorithm shows that the model for optimal headway is used in determining the motion goal of the vehicle and in calculating its safety function. The motion goal of the vehicle determines how far it will travel in the timestep, and the safety function determines the lane of travel for the vehicle. Therefore, we decided the first step toward optimizing the performance of CATS was to calibrate the input parameters of the model for optimal headway. Referring back to Figure 1, this model defines the optimal headway as a function of the vehicle speed. The input parameters that need to be calibrated are the initial slope  $\alpha_1$  (the rate of increase of headway when vehicle speed is between 0 and  $S_r$ ) and the reference speed,  $S_r$ . These parameters will have the greatest effect on optimal headway calculations. The headway at rest ( $G_0$ ) is set at 1 foot, and the second slope  $\alpha_2$  is set to 0.0 because it is assumed that after  $S_R$  has been reached, the optimal headway will remain constant regardless of the vehicle's speed. The CATS model is run with different combinations of values for  $\alpha_1$  and  $S_r$ , and the results are compared to field data by using the conservation metric  $Q$  and the flow density plots described in Section 3.3.

The range of  $S_R$  values was set between 30 and 80 mph, and the range of  $\alpha_1$  values was 1 to 3 feet/mph. The percentage difference in car conservation between the model and the field data for each combination of input parameters was computed and is illustrated in the bar graph of Figure 13. These results indicate that  $\alpha_1 = 2.5$  feet/mph gives the minimum percentage difference (1.1%), regardless of the value of  $S_R$ . This means that on average, the CATS model contains 1 percent more cars than the actual highway.

Using these results, the next step was to determine the optimal  $S_R$  value for  $\alpha_1 = 2.5$  feet/mph by comparing and analyzing the flow versus density plots. An examination of the existing literature found that other authors visually compared the basic characteristics of the flow versus density plots. A more quantitative approach was taken here by using the methods outlined below. The flow versus density plots generated by the CATS model using  $S_R = 30, 45, 60, 70,$  and 80 mph and the field data are illustrated in Figure 14. These plots show that flow first increased with density until a maximum was reached, and from there flow decreased with increasing density. The flow values increased in discrete steps because they were initially reported by the sensors in

integer units of vehicles/20 seconds and then converted to vehicles/hour. Comparing the flow versus density plots generated by the field data and the model, we observed that the maximum model density was less than the maximum field density at each discrete flow value. It is difficult to model highly congested traffic, and therefore, the best  $S_R$  value is the one that can produce the highest density at each flow. After further analysis of the flow versus density plots, we proposed that this observed maximum density ( $D_{max}$ ) at each flow value could be modeled as the sum of a deterministic and random component. The deterministic component depends on the flow ( $v$ ) and is represented by the following equation:

$$D_{max}(v) = cv \quad (15)$$

where  $c$  is a constant that represents the slope of the maximum density versus flow line.

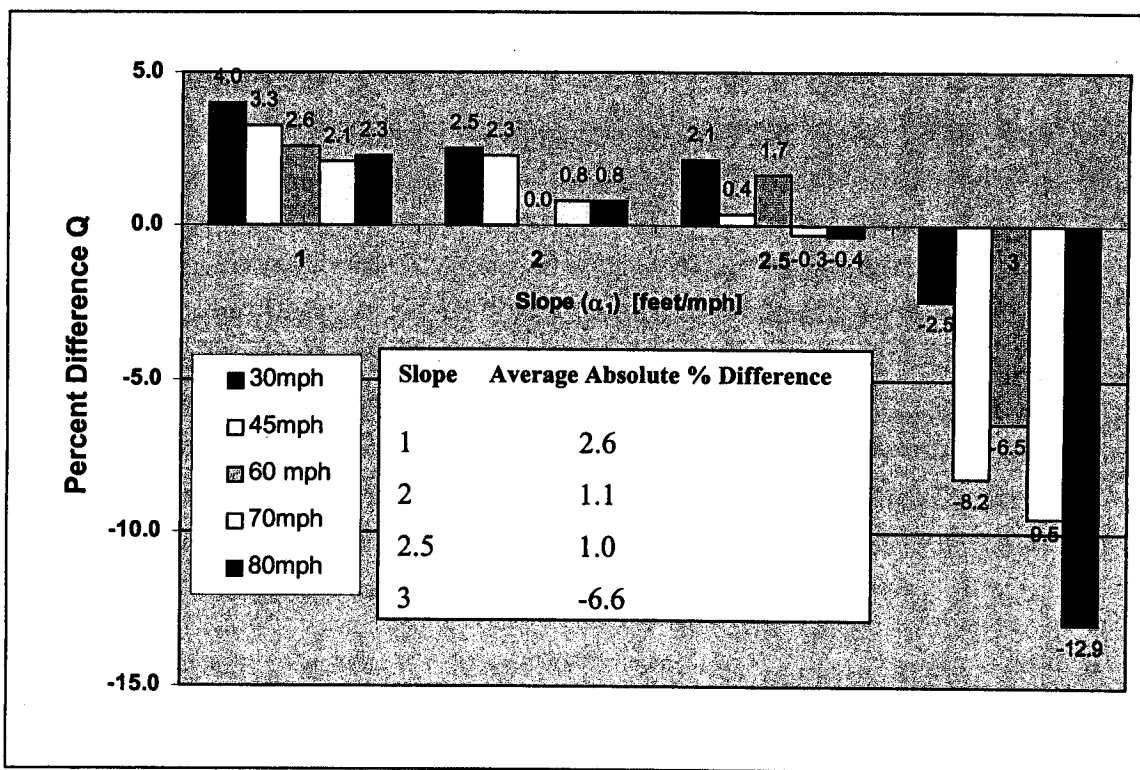


Figure 13: Comparison of conservation of cars between model and field data using different values for input parameters in the model for optimal headway.

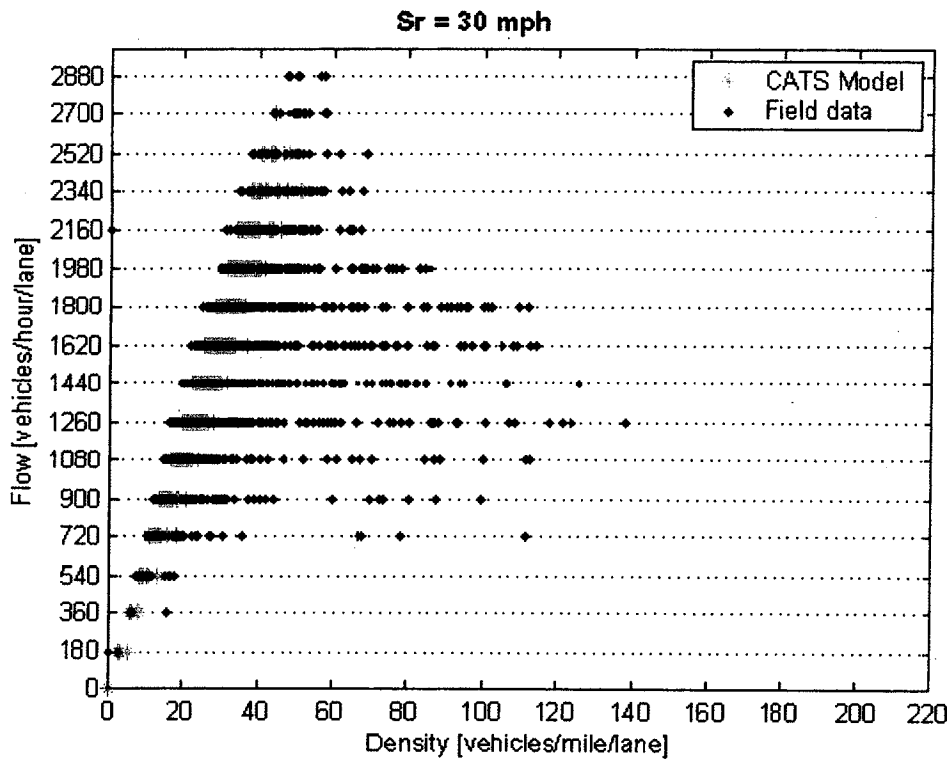


Figure 14: Flow versus density plots for varying  $S_R$  values.

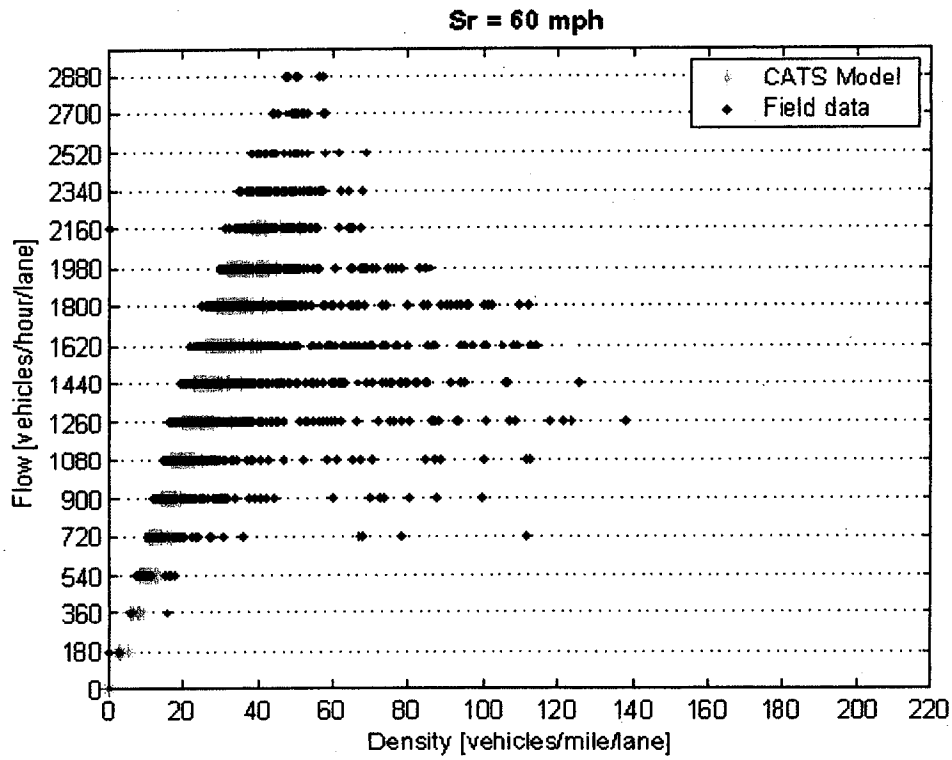


Figure 14 (continued): Flow versus density plots for varying  $S_R$  values.

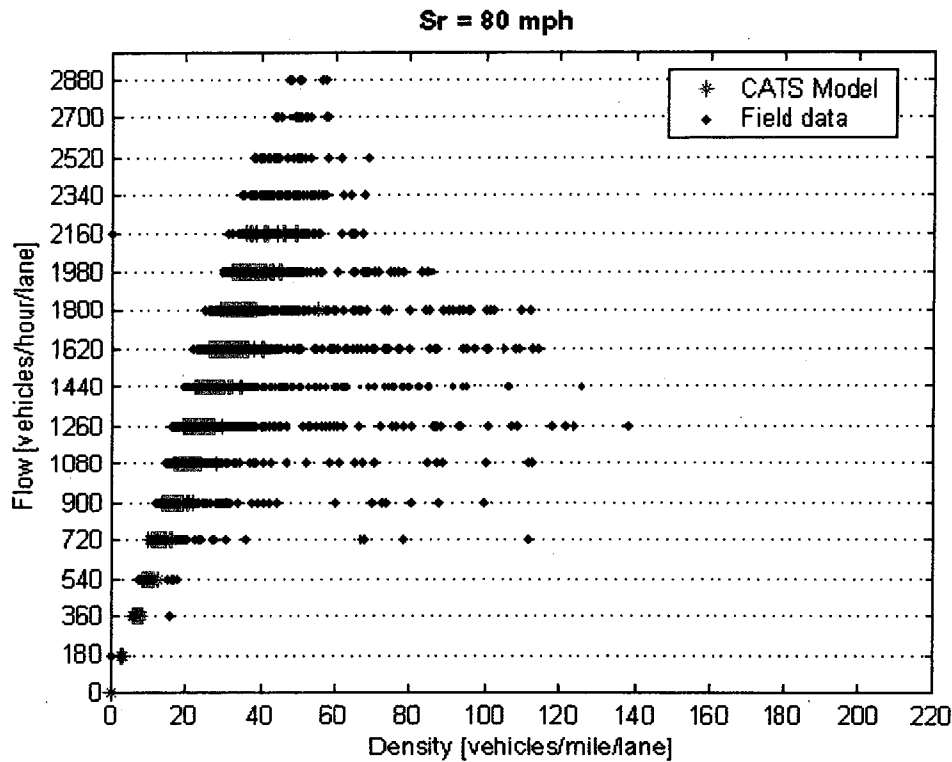


Figure 14 (continued): Flow versus density plots for varying  $S_R$  values.

The random component,  $\delta(S_R)$ , represents the component of maximum density that depends on the specific  $S_R$  value used in the simulation. Therefore, the maximum density for a particular flow and reference speed is

$$D_{\max} = cv + \delta(S_R) . \quad (16)$$

To calculate the  $c$  value, the maximum density at each flow for all  $S_R$  values was plotted, and a line was fit through the data using a least squares method, as shown in Figure 15. The slope of the line or  $c$  value was 0.0231 hours/mile.

To determine which value of  $S_R$  would give the maximum density at each flow value,  $\delta$  for all  $S_R$  values was plotted, as shown in Figure 16. A polynomial curve was fit through these data points to find the relationship between  $S_R$  and  $\delta$ . The resulting equation was

$$\delta = -0.0016S_r^2 + 0.2093S_r - 3.8788 . \quad (17)$$

The derivative of equation (16) was set to 0.0 to find the  $S_R$  value that would result in the largest  $\delta$ ,

$$\frac{\partial \delta}{\partial \delta_R} = 2x - 0.0016 \times S_R + 0.2093 = 0 \quad (18)$$

Solving equation (18) gave  $S_R = 65.41$  mph. Therefore, the best parameters for the model for optimal headway were  $\alpha_1 = 2.5$  feet/mph and  $S_R = 65.41$  mph. To verify these results, a flow versus density plot was generated by the CATS model using these parameter values, as shown in Figure 17. A visual comparison of this plot with the previous ones in Figure 14 showed that the CATS model was able to model the high-density conditions with these input parameters. Also, the percentage difference in cars between the model and field data for these input values was only 0.8 percent. In summary, the conservation of cars metric and a comparison of the plots of traffic flow versus density were used to find the input parameters that resulted in the best performance of the CATS traffic simulation model

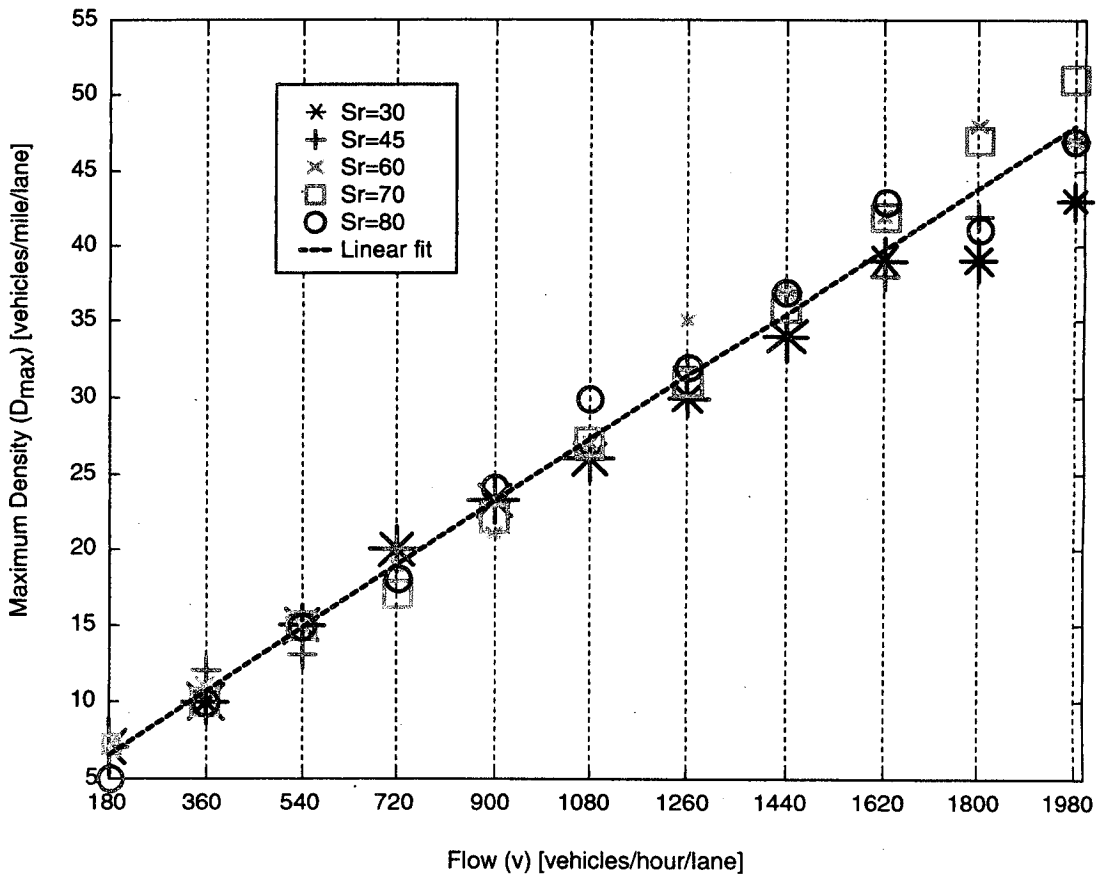


Figure 15: Maximum density versus flow for each  $S_R$  value.

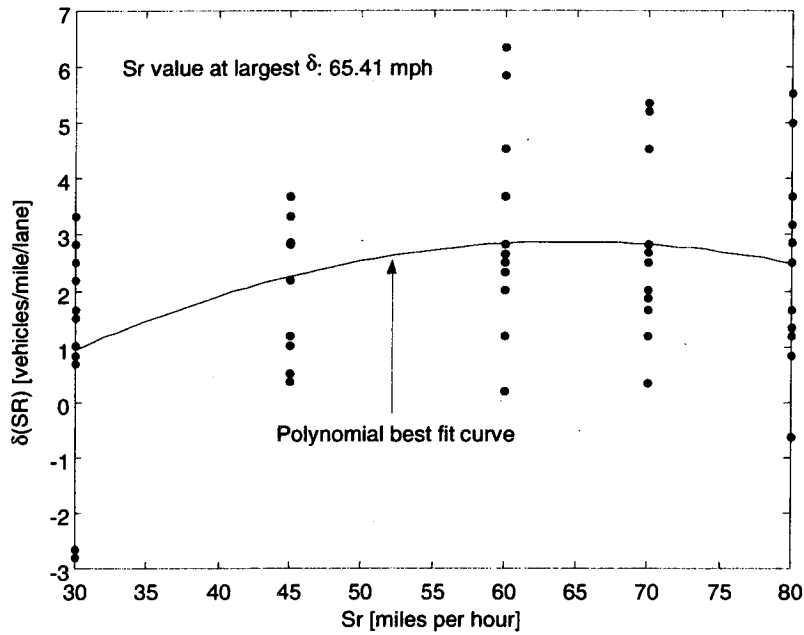


Figure 16: Random component of  $\delta$  versus  $S_R$  with polynomial best fit curve.

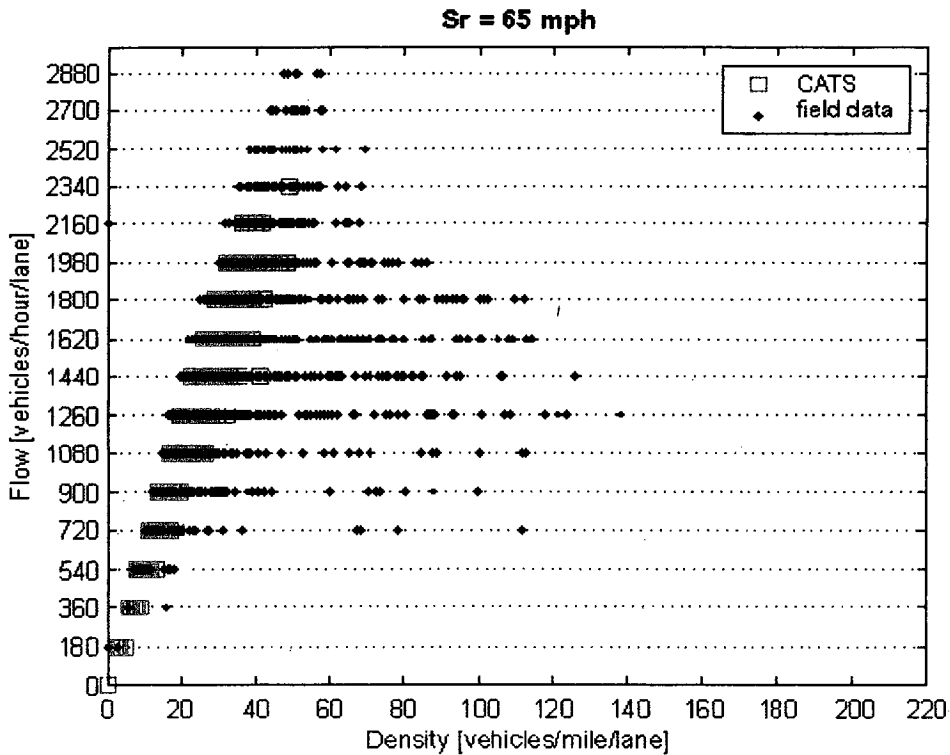


Figure 17: Flow versus density plot for optimal  $S_R$  value.

#### **4. CONCLUSIONS AND FUTURE WORK**

This report presents a model for traffic flow simulation and prediction. The model uses cellular automaton theory to model complex traffic behavior. The advantage of the cellular automata approach is that the roadway to be modeled is quantized into simple homogeneous cells, time is quantized into discrete steps, and physical quantities take on a finite set of values. Also, the state of the cells is updated at discrete timesteps by using a vehicle update algorithm that combines a few vehicle motion models that are governed by a relatively small set of parameters. This allows the model to be calibrated easily and also allows the simulation to run very fast. CATS can simulate traffic flow on the road in under 2 percent of the actual time period being simulated.

Using volume data from traffic sensors embedded in the access and exit ramps of the highway as boundary conditions, the model predicts traffic flow on the mainlines at points farther downstream. To evaluate the accuracy of CATS, the observed volume and occupancy measures can be compared directly with field data from traffic sensors on the road. The extensive comparison of the calculated results with field data is one of the key difference between CATS and existing models.

To evaluate the model's performance, it is used to simulate southbound traffic on an 11-mile section of I-5 in Seattle, Washington. A simulation period that covered a broad range of traffic conditions was chosen to ensure that the model was being tested for all levels of congestion. A method parameter calibration was presented, using the model for optimal headway as an example. This model was chosen because it has the greatest impact on the vehicle position update algorithm. CATS was run repeatedly for the same simulation period and roadway using different values of input parameters. The results from the model were evaluated with a conservation of cars metric and plots of traffic flow versus density. These metrics were compared, and the best values for the input parameters were chosen accordingly. The comparison showed that running CATS with these input parameter values did indeed increase the accuracy of the model and that CATS was able to accurately predict vehicle behavior on the freeway.

To completely optimize the accuracy of the model, all the input parameters used in the vehicle motion models need to be calibrated. In addition, the parameters can be calibrated more formally by using optimization methods. The next phase of this project will develop the necessary



optimization techniques as well as modify the model to have a finer granularity in time and space. This will result in a General Automata suitable for congestion prediction.

Some features that may be added to improve and extend the capability of this model include the following:

- a driver behavior factor to improve the vehicle description
- ability to specify the time and location of lane accidents or construction work
- support for reversible express lanes
- ability to assign origin-destination pairs to the vehicles.

In addition, the usability of CATS may be enhanced by adding a graphical user interface so that a user can easily modify the simulation setup and input parameters. Future direction for the model may also include an improvement of the vehicle position update algorithm to increase the accuracy of the model on a microscopic level.

There are large potential benefits to a variety of traffic information and management activities if accurate traffic condition prediction can be done over a large region. Changes to geometry as well as congestion can be simulated using the proposed technique so that arenas ranging from planning to traveler information can benefit. For example, the types of planning questions that might benefit from such modeling are as broad as the effect of lane closures for maintenance, the time of day for such maintenance, to changes in HOV policy or incident response resource allocation. The traveler information benefits range from prediction for route decisions to estimates of incident clearing times. The accurate prediction of detailed traffic behavior opens the door to a new genre of route guidance, fleet management, and transit management and advance traveler information systems possibilities on a regional and national scale.

Creating a model that accurately predicts future congestion based on the physics of traffic provides a foundation for real-time, optimal control as well as providing a powerful test bed for modeling roadway capacity changes such as lane closures and incidents. This proof of principle activity on I-5 North can contribute a predictive capability to the ramp control activity already underway at WSDOT TSMC, as well as providing the framework for a combined freeway and arterial control system.

As the number of vehicles on the roads continually increases, the ability to accurately simulate traffic flow is becoming more important so that existing highways can be improved and better road geometries can be designed in the future.

A paper was presented on this topic at the Transportation Research Board 80th Annual Meeting, January 7-11, 2001, in Washington, D.C., and is included as Appendix A.

## REFERENCES

1. Chronopoulos, A.T. and C.M. Johnston. A Real Time Traffic Simulation System. *IEEE Transactions on Vehicular Technology*, Vol. 7, No. 1, pp. 321-331, February 1998.
2. May, A.D. *Models for Freeway Corridor Analysis*. Technical Report, National Academy of Sciences, Spec. Rep. 194, 1981.
3. Ziliaskopoulos, A. and S. Lee. A Cell Transmission Based Assignment-Simulation Model For Integrated Freeway/Surface Street Systems. Transportation Research Board 76<sup>th</sup> Annual Meeting, January 1997.
4. *CORSIM User Manual Version 1.01*, U.S. Department of Transportation, Federal Highway Administration, Washington D.C. August 1996.
5. Prevedouros, P.D. and Y. Wang. Simulation of Large Freeway and Arterial Network with CORSIM, INTEGRATION, and WATSIM. *Transportation Research Record*, Vol 1678, pp. 197-207, 1999.
6. Smith S., R. Worrall, D. Roden, R. Pfefer and M. Hankey. *Application of Freeway Simulation Models to Urban Corridors Volume I: Final Report*. U.S. Department of Transportation, Federal Highway Administration FHWA-RD-92-103, Washington D.C., 1992.
7. Daganzo, C. The Cell Transmission Model: A Dynamic Representation of Highway Traffic Consistent with Hydrodynamic Theory. *Transportation Research B.*, Vol. 28B, No.4, pp. 269-287, 1994.
8. Daganzo, C. The Cell Transmission Model Part II: Network Traffic. *Transportation Research B.*, Vol. 29B, No. 2, pp. 79-93, 1995.
9. Cayford, R., W. Lin and C. Daganzo. *The NETCELL simulation package: Technical Description*. California PATH Research Report, UCB-ITS-PRR-97-23, 1997.
10. Nagel, K. and M. Schreckenberg. A Cellular Automaton Model for Freeway Traffic. *Journal de Physique I France*, Vol. 2, pp. 2221-2229, 1992.
11. Wagner, P. , K. Nagel and D. Wolf. Realistic multi-lane traffic rules for cellular automata. *Physica A*, Vol. 234, pp. 687-698, 1997.

12. Esser, J. and M. Schreckenberg. Microscopic simulation of urban traffic based on cellular automata. *International Journal of Modern Physics C*, Vol. 8, No. 5, pp. 1025-1036, 1997.
13. Schreckenberg, M., A. Schadschneider, K. Nagel and N. Ito. Discrete Stochastic Models for Traffic Flow. *Physical Review E*, Vol. 51, No. 4, pp. 2939-2949, 1994.
14. Nagel, K., D. Wolf, P. Wagner and P. Simon. Two-lane traffic rules for cellular automata: A systematic approach. *Physical Review E*, Vol. 58, No. 2, pp. 1425-1437, 1998.
15. Rickert, M., P. Wagner and Ch. Gawron, Real-Time Traffic Simulation of the German Autobahn Network. Report No. 1997.309, *Proceedings of the 4<sup>th</sup> Workshop on Parallel Systems and Algorithms*, 1996.
16. Wolfram, S. *Theory and Applications of Cellular Automata*. World Scientific, 1986.
17. Von Neumann, *Collected Works*, 1963.
18. Fathy, S. Some ideas and prospects in biomathematics. *Ann. Rev. Bio.*, page 255, 1974.
19. Creamer, M. and J. Ludwig. A fast simulation model for traffic flow on the basis of Boolean operations. *Mathematical and Computers in Simulation*, Vol 28, pp.297-303, 1986.
20. Fuks, H. Exact Results for deterministic cellular automata traffic models. *Physical Review E*, Vol 60, No. 1, pp. 197-202, 1999.
21. Nsour, S. and A. Santiago. Comprehensive Plan Development for Testing, calibration and validation of CORSIM. *Compendium of Technical Papers, 64<sup>th</sup> ITE Annual Meeting*, pp. 486-490, 1994.
22. Aycin, M.F. and R.F. Benekohal. Comparison of Car-Following Models for Simulation. *Transportation Research Record*, Vol 1678, pp. 116-127, 1999.
23. Wagner, P. Traffic Simulation Using Cellular Automata: Comparison with Reality. *Traffic and Granular Flow Conference Proceedings*, Report No. 95.214, 1995.
24. Lieberman, E. and A. Rathi. Traffic Simulation. *Transportation Research Board Special Report 165, Traffic Flow Theory*, 1992.

25. McShane, W.R., R.P. Roess and E.S. Prassas. *Traffic Engineering Second Edition*. Prentice Hall, New Jersey, 1990.
26. *Highway Capacity Manual Special Report 209*. Transportation Research Board, National Research Council, Washington, D.C., 1985.
27. Salter, R.J. and N.B. Hounsell. *Highway Traffic Analysis and Design Third Edition*. Macmillan Press, London, 1996.
28. Greenshields, B. *A Study of Traffic Capacity. Proceedings of the Highway Research Board*, Vol. 14, Transportation Research Board, National Research Council, Washington, D.C., 1934.

## **APPENDIX A**

### **PAPER NO. 01-3034: A GENERAL AUTOMATA CALIBRATED WITH ROADWAY DATA FOR TRAFFIC PREDICTION**

Z. Wall, R. Sanchez\*, D.J. Dailey  
University of Washington  
Department of Electrical Engineering  
Box 352500  
Seattle, Washington 98195-2500  
206-543-2493  
206-616-1787 fax  
dailey@ee.washington.edu

\*DMT/SERMA,  
CEA de SACLAY  
91191 GIF-SUR-YVETTE CEDEX  
FRANCE

#### **ABSTRACT**

We present a microscopic model of traffic flow with the intent of using the model in conjunction with real-time inductance loop sensor data to predict downstream traffic volumes and speeds. We calibrate the model such that the output of the model and the observed loop data match in a least squares sense. The model parameters are determined using a line search on a least squares cost function with a Newton's method update and a finite difference differential approximation. Once the model is calibrated, the output of the model is experimentally validated using observed roadway data. The differentiating feature of this work is the manner in which the loop inductance data is used to calibrate and validate the microscopic model parameters and the consequential predictive ability of the model. Past work in the literature does not use historical data calibrate model parameters in an iterative process, whereas the present work optimizes the model parameters using real traffic data from a variety of conditions.

#### **INTRODUCTION**

Traffic flow modeling is an integral part of any traffic control system. Since traffic flow is a granular flow process, it can be modeled using microscopic techniques (in addition to standard macroscopic techniques). While there have been many successful macroscopic models (e.g. [1] [2] [3] [4] [5]), the desire to represent the diversity of the 'realistic' road performance using a short

time scale has given rise to the development of a number of microscopic models in the last few years. Theoretically, every aspect of the environment, driver, and car can be modeled using a microscopic model, but in practice, most models are very simple because of difficulties associated with having a large parameter space.

A typical microscopic model considers the current vehicle, driver behavior, road geometry, and surrounding vehicles (those within the driver's perception) while determining the next 'state' of the vehicle. Each driver/vehicle combination in the traffic may be described by a set of parameters such as position, actual speed, route choice, driving style, etc. While the simplest microscopic models can be described using analytic equations [6], as model complexity increases, it is difficult to precisely derive the equations necessary to describe microscopic traffic phenomenon. This is due to the complexity, randomness, and interdependency of the processes involving vehicles on the roadway. As a result, computer simulations, rather than analytic models, are the primary means of implementing microscopic models ([7] [8] [9] [10] [11]).

Recently, Nagel et al proposed a multi-lane microscopic model that uses a stochastic discrete automata model [9]. Automata networks comprise some of the most powerful tools for modeling natural, dynamic systems on a computer. An automata network is described by three main components: a set of vertices, an interconnection graph, and the transition function for each vertex [12]. One of the most basic forms of automata networks is the cellular automata (CA) network. A CA network is a subset of an automata network with the following restrictions: the interconnection graph must be a cellular space (each vertex can only connect to its closest neighbors) and the transition function must be translation invariant. These models have shown much promise in the ability to reproduce many complex traffic phenomena (such as shockwaves). The work presented here builds upon the discrete automata framework with a number of key improvements

## **MODEL DESCRIPTION**

A primary result of a CA network definition is that each cell is updated synchronously (in parallel). While this has many computational benefits, it also has the limitation that certain state transitions cannot occur because of conflicts with occupied cells further down the road. These 'garden of eden' states are a limitation of CA models because they alter the way that the cars propagate down the road [13]. However, the general automata (GA) network allows for a

sequential update pattern. As a result, a GA model can move downstream cars first so that the upstream cars have a place to move, eliminating the 'garden of eden' states.

In a CA network, each cell must completely account for the size and stopped headway of a car. This is a requirement because it is the only way to ensure that each cell has identical transition rules. However, the GA network does not have to maintain identical transition rules so it is possible to reduce the size of each cell. This fact leads to a number of important advantages in the GA model compared to the CA model.

In a GA model, the size of a cell is arbitrary and can be set to relatively small values (typically 4 feet or less in our model). This increases the model resolution. As a result, the GA model is able to match the actual distribution of vehicle speeds much more closely than a typical CA model. The smaller cell size also is an important factor in car choice. In the GA model, we can have multiple car types and lengths because a car can occupy more than 1 cell. This allows us to create a model of traffic that represents the actual distribution of cars on the freeway more closely than the CA model. Along with the increase in velocity resolution, we are able to model both differences in car speed and length.

Another important advantage of the GA model is the ability to create location dependent transition functions. When modeling on and off ramps, the GA model has the ability to assign different probabilities for exiting/entering the freeway based on the location of the ramp in question. This allows for a more realistic representation of traffic flow on the freeway than is possible with the CA model.

The combination of multiple car types and location-based transition probabilities allows for HOV analysis that is difficult with a CA model. Specific car types that are designated as HOV capable vehicles can be introduced into the model and then use HOV lanes with specific lane changing probabilities based on the actual geometry of the freeway.

While previous CA models are forced to use a very simple model for the driver and roadway because of the limitations of the CA network framework, our GA model is able to handle a more complex array of parameters. As a result, we are able to incorporate parameters derived from real highway data directly into the model.



The result of these improvements is a discrete automata model that has a rich feature set comparable to existing state-of-the-art microscopic models. The model presented here has the ability to represent multi-lane freeway traffic behavior including on/off ramps (with metering), turning percentages, multiple car types, special consideration for HOV lanes, and multiple driver models. The extension of the discrete automata framework to include this rich feature set is necessary to handle the effects of incorporating real data.

While one of the target applications of the current generation of microscopic models is the quantification of the benefits of Intelligent Transportation Systems [14], our traffic flow model also has the ability to perform real-time traffic flow prediction. While others have proposed neural networks to perform traffic flow prediction [15], the neural network representation relies on basis functions generated from historical data and, as such, relies heavily on the notion that the traffic flow time series is stationary. This sort of prediction algorithm has difficulty when traffic flow deviates from the norm due to unforeseen conditions (weather, traffic incidents, etc.)

The primary differentiating feature of the model presented here is the methods used to incorporate real data into the model. While other microscopic models often apply parameters calculated from a generic set of traffic data, the model presented here uses roadway-specific data to calibrate and verify the model. Using traffic volume and occupancy data collected from loop inductance sensors, a roadway specific set of parameters is calculated. Additional parameters (such as car length and target speed) are calculated using speed trap information.

During the operation of the model, real data is used to enforce the boundary conditions at the on and off ramps. This ensures that the number of cars entering the road matches the situation being modeled. Other microscopic models ([10] [11]) typically use turning percentages to perform this operation. However, the addition of random process for the boundary conditions to model on and off ramp behavior means that the output of the model matches the loop data in the least squares sense.

The model is calibrated by adjusting the parameters to match the stochastic time series from the individual loop sensors in the least squares sense.

The verification process of the model is accomplished by monitoring the flow of cars at the 'end' of the model. Since the cars can only enter the model via the ramps, the behavior of the

model at the end represents the result of the simulation. The simulated traffic flow time series for the downstream location is compared to real data from the corresponding loop sensors using both traffic flow analysis techniques and stochastic analysis techniques.

We present an implementation of a discrete automata model that simulates traffic flow on a freeway. By calibrating and verifying the operation of the model using loop inductance data, we create a simulation that has the ability to predict downstream traffic behavior at a later time when given upstream/earlier inductance loop data as input.

## **IMPLEMENTATION**

The general automata model we construct is designed to simulate an open-ended multilane roadway. In the model, a fixed length of roadway is represented by a number of fixed length cells. This is similar to the cellular automata model described in [8] and [9] where the roadway is also described by fixed length cells. However, in the CA description, each cell is sized such that it will exactly contain one vehicle. In our model, the choice of cell length is arbitrary in that we allow a vehicle to span multiple cells. The cell length determines quantization of the speed, density, and vehicle length. By using a small cell size (in our experiments, 8 feet), the effects of quantization are reduced compared to the typical 22-foot cell size used by CA models. This ability to reduce cell length to the point that quantization effects are minimal is a key feature of the model.

Another byproduct of using a GA model is the ability to assign different rules to cells during the same processing pass. In contrast, in a CA model every cell must use the same set of rules during a particular processing pass. As a result, a CA model of a road typically is ring shaped such that there is no entrance or exit.

On or off ramps and HOV lanes are designated by changing the rule set assigned to a particular cell. The model is able to support a wide number of road geometries. The number of lanes and the total length of the road are only limited by the capacity of the computer. On and off ramps are modeled using cells with the added function of being able to add or subtract cars from the road. The model also has support for reporting simulated inductance loop output. This allows a user to compare the output of a simulation to existing records of the freeway.

The driver model is similar to earlier CA driver models by Nagel and Schreckenberg [16]. For single lane car following, our primary driver goal is to maintain a safe headway with the car in front. Based upon the headway calculation, the driver will perform actions including breaking and lane changing.

While the CA rule set is designed for parallel operation, our GA rule set is design for sequential operation. Downstream cars are moved first, clearing space for the upstream cars to move into. The goal of our driver is to reach and maintain an optimal headway while travelling at the target speed. Every timestep, the headway is checked and a decision is made (accelerate, brake, maintain speed) based upon the current position in relation to nearby cars.

For multilane operation, the lane-changing model is an extension to one presented by Nagel [9]. While the CA model lane uses an additional step to perform the lane changing operation, the GA driver model is able to move the car forward and change lanes at the same time. This is accomplished by propagating the car forward as a test and then checking the gaps between the cars in the left or right lanes to determine if there is enough space to change lanes. If a space exists in the new lane (within a safety margin), the car will change lane with a certain probability.

Our multilane operation is further extended by the ability to locally adjust the lane change probabilities due to external factors such as ramp location. A cell can be designated as being upstream or downstream of a ramp. Cells with this designation have an additional lane changing probability term associated with them. This causes cars to change to/from the ramp more frequently depending on the situation.

Another aspect of the ability to assign different rulesets to individual cells is the ability to model a wide range of vehicles. The size and performance characteristics of a vehicle are parameters in the model. Any number of cars with a variety of parameters can be described. A distribution function is used to determine which type of vehicle is added to the model during run time. In this way, our model begins to represent the variety of cars found on a typical freeway. This also allows us to model HOV operation. A certain percentage of cars can be given the 'HOV' designation. Cars with this flag have the ability to change into the HOV lanes if they desire.

## CALIBRATION

We present a roadway model for an eight-mile stretch of Interstate 5 in Seattle, Washington. This model contains the topology of the road as defined by the surveillance system used to collect data. A schematic of a subsection of this topology is shown in Figure 1. Every on-ramp and off-ramp is accounted for and associated with a specific sensor data that can be extracted from a data mine of roadway data. The first mainline sensors encountered are treated as inputs to the model just as the on-ramps are.

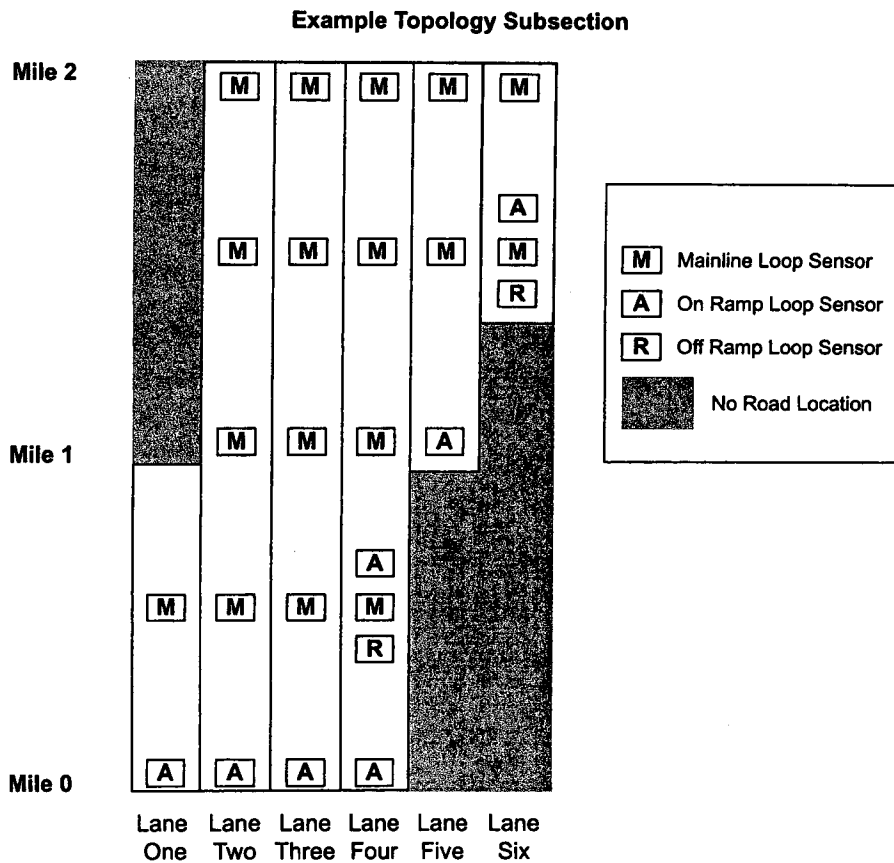


**FIGURE 1 Topology schematic.**

The combination of the topology and a corresponding inductance loop data set form the basis of the analysis of the model. The data set represents the observed traffic flow on the road during a specific time interval. Recognizing the fact that the traffic flow is a time varying process, we choose a time interval where the flow transitions through a wide range of different states of

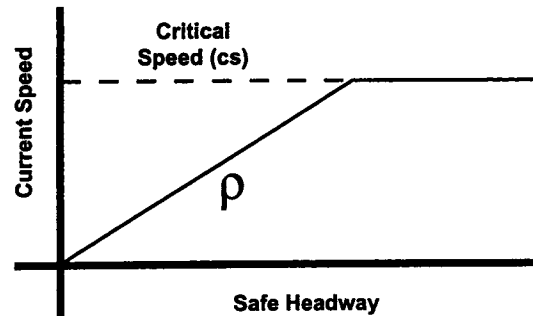
congestion. The wide range of congestion states ensures that our parameter analysis and optimization routines are run using a variety of different traffic conditions. As a result, the optimized parameters will represent the best possible settings for the model to predict the traffic flow under normal operating conditions.

To optimize the parameters, a cost function is used. This cost function evaluates the performance of the model by comparing its behavior to the actual traffic. There are three performance criteria that are incorporated into the cost function. The first criterion is the ability of the model to match the boundary conditions specified by the historical data. The second criterion is a comparison between the volume of cars measured by the set of inductance loops at each time step and the output of the simulated inductance loops from the model. The final comparison is between the average exit speed from the model and the average speed of the cars as recorded by a speed trap sensor at the location of exit. The average exit speed metric evaluates the performance of the model as a predictor. In essence, given a flow of cars at one point on the freeway, the model predicts the average speed of the cars at some downstream location (and the link travel time). These three criteria, evaluated in a least squares sense, are summed into a single cost function or metric that weighs the overall operation of the model.

For the results presented in this paper, we choose to fix the vehicle parameters and focus on the driver parameters. The vehicle parameters, length, willingness to speed, acceleration rate, HOV usage, and braking rate, were set using empirical data and engineering judgement. The vehicle types included one HOV vehicle, two types of passenger vehicles, and one type of commercial vehicle.

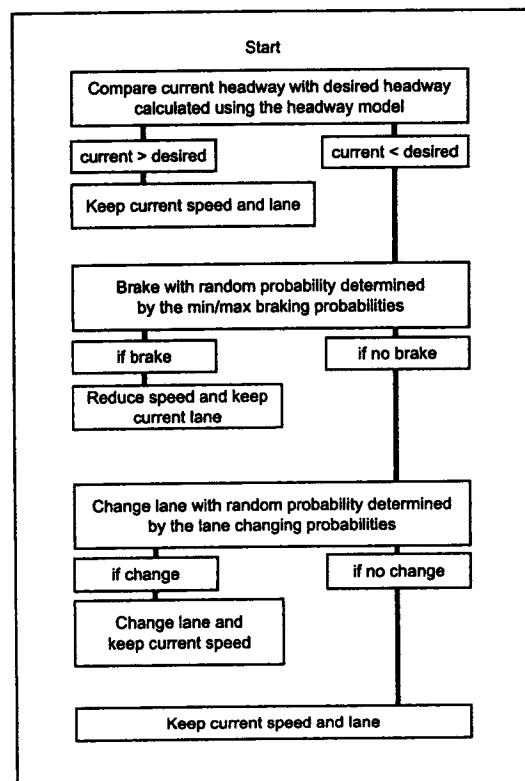
Six parameters are examined: a two-parameter headway model as shown in Figure 2, two asymmetrical lane changing probabilities, and two breaking probabilities. The headway model is used in the first step of the driver behavior tree. A driver's desired headway is calculated using the point (critical speed) – slope ( $\rho$ ) parameters of the headway model. Depending on the difference between the desired headway and actual headway, the driver will perform different actions (change lane, change speed, etc.) as shown in Figure 3. These parameters directly affect the limits of the flow of vehicles through the model. The asymmetrical lane changing probabilities govern the tendency of a driver to change lanes in order to increase speed. The min/max breaking

probabilities govern the tendency of a driver to brake given his current headway. If the current headway is too small for the current speed, the driver will brake according to these probabilities.



**FIGURE 2 Headway model.**

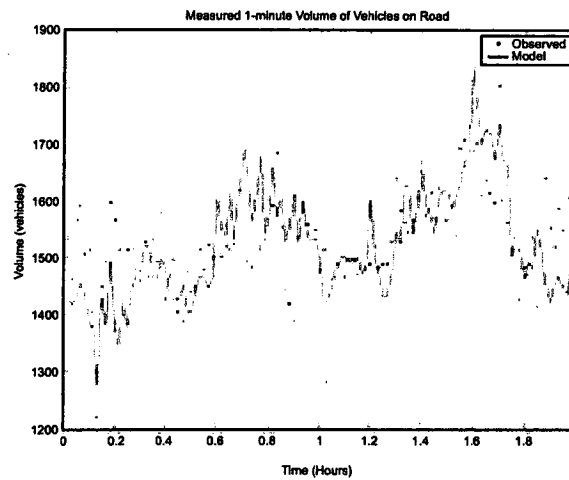
Using the inductance loop data, the model, and the vehicle parameters, we optimize the driver parameters to minimize the metric. Since the model does not have an analytic form, we used a line-search with a Newton's update and a finite difference differential approximation.



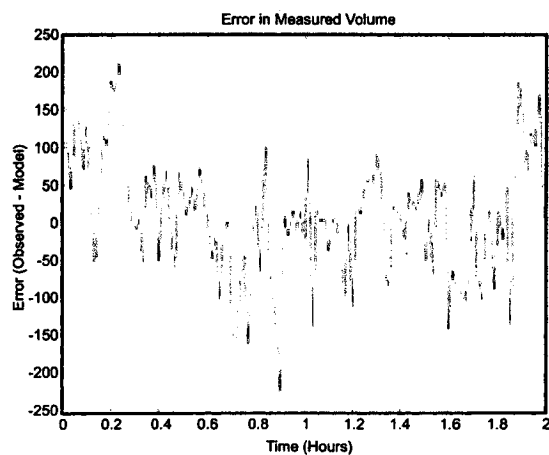
**FIGURE 3 Algorithm flow diagram.**

## VERIFICATION

To validate the model, we compare the output of the model to inductance loop data. The comparison is between the one-minute measured volumes for each inductance loop and the model simulation of an inductance loop sensor at that location. Figure 4 shows the time series for both the measurement and the simulation for every loop location over a two-hour period. At any given time step, the measurement and the simulation differs by less than 10%. Figure 5 shows the deviation between these two time series. The time series shown are correlated with a cross-correlation coefficient function evaluated at zero lag (CCF) of  $\sigma_{xy} = .54$ .

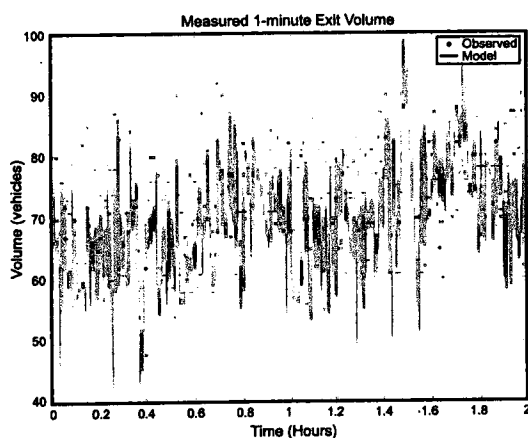


**FIGURE 4 Measured and simulated volumes.**

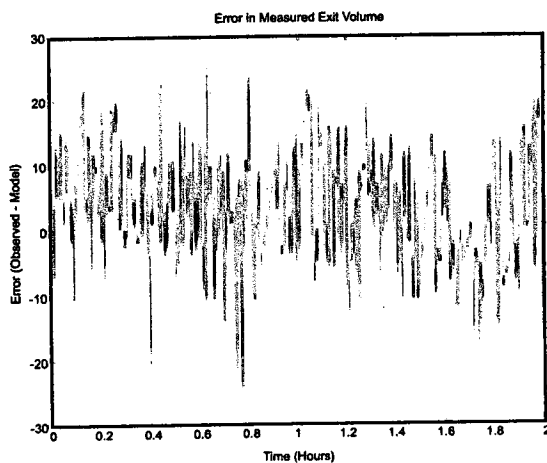


**FIGURE 5 Deviation of measured data from simulation.**

In addition, we compare the measurement and simulations of the volumes of vehicles exiting the model in one minute. The exit flow volume is the only boundary condition that is not directly fixed to the historical data. This exit volume is the predicted volume of cars exiting the model given that the upstream boundary conditions are satisfied. Figure 6 shows the time series for both the measurements and the prediction of the exit volumes. Figure 7 shows the deviation between the measurement and the simulation of the exit volumes. These two time series are correlated with a CCF of  $\sigma_{xy} = .44$ . The mean of the deviation between the exit volumes is near zero vehicles and has a standard deviation of 7.9 vehicles.



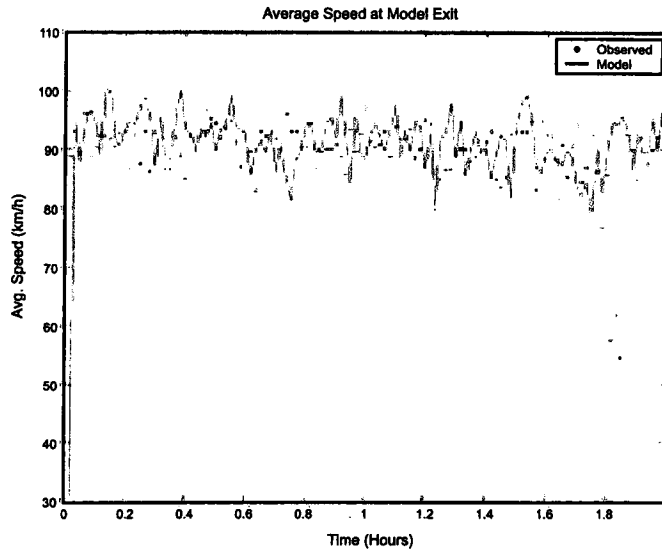
**FIGURE 6** Exit volumes.



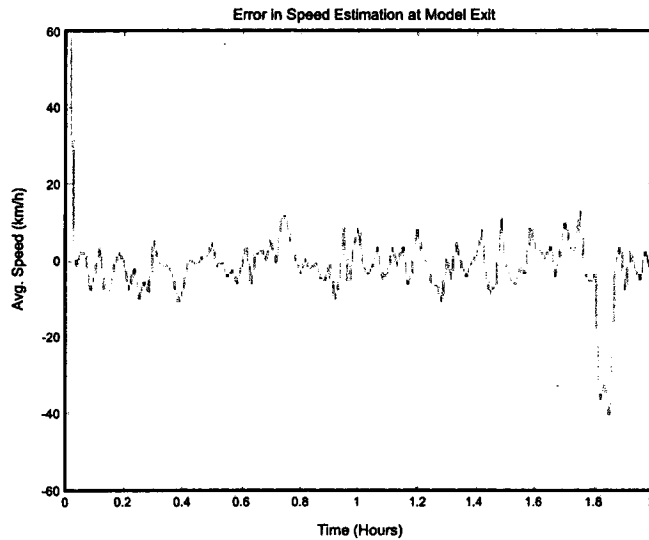
**FIGURE 7** Deviation of simulated and measured exit volumes.



Figure 8 shows the both the measured and predicted average speeds at the output of the model. The mean value over time of these two stochastic processes is approximately equal as shown by the deviation between the two time series in Figure 9.



**FIGURE 8** Speed comparison.



**FIGURE 9.** Deviation of simulated speed from measured speed.

As a final means of evaluating the model, we compare the resulting flow-density diagrams as suggested in [9]. Figure 10 shows the flow-density diagrams for both the model and the historical data over the same two-hour time period. The similarity between the two diagrams suggests that the level of congestion of the model matches the level of congestion on the actual roadway during the test period.

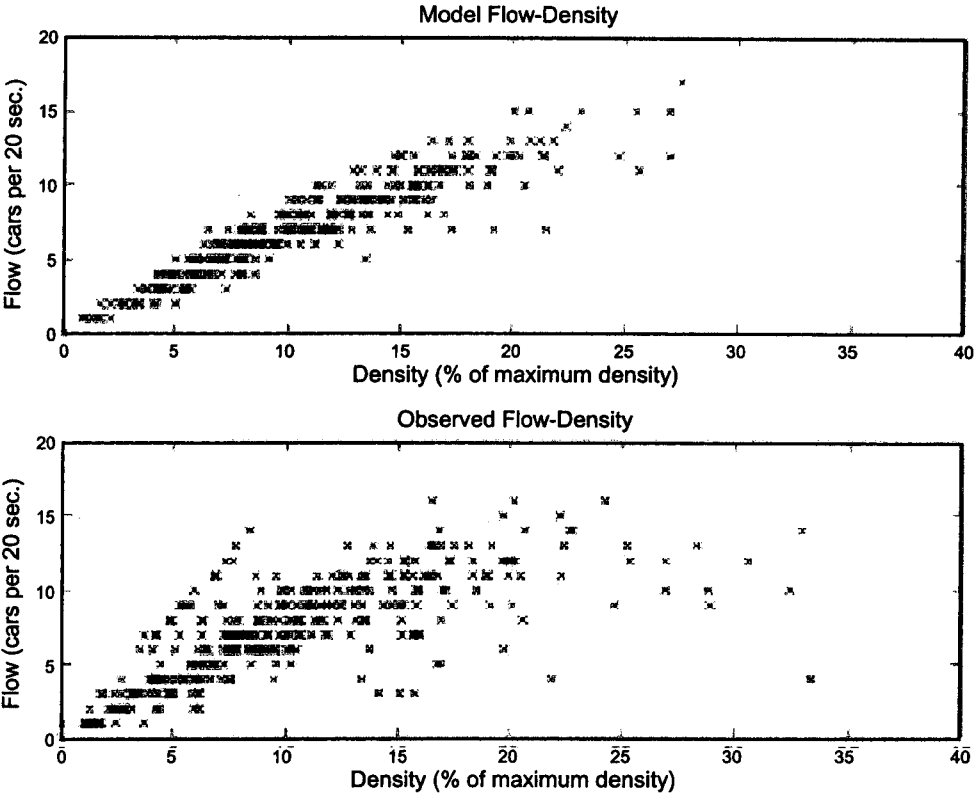


FIGURE 10 Flow-density diagrams.

**CONCLUSION**

This paper presents a microscopic model of vehicle behavior with the intent of using the model in conjunction with real-time inductance loop sensor data to predict downstream traffic volumes and speeds. We calibrate the model such that the output of the model and the observed loop data match in a least squares sense. The model parameters are determined using a line search on a least squares cost function with a Newton's method update and a finite difference differential approximation.

In general, the exit volume predicted by the model is correlated with the volume of cars recorded by the sensors. Moreover, the volumes and congestion levels found in the model are similar to the historical volume and congestion. Future work includes refining the model to be able to predict the exit speed directly and improving the methods of incorporating loop inductance data such that missing data is less of the problem.

## ACKNOWLEDGEMENTS

This work was supported in part by a series of contracts with the Washington State Department of Transportation and by the U.S. Department of Transportation.

## REFERENCES

1. Daganzo, C. Requiem for Second-Order Fluid Approximations of Traffic Flow. *Transportation Research Part B*, Vol. 29B, No. 4, August 1995, pp. 277-286.
2. Daganzo, C. A Continuum Theory of Traffic Dynamics For Freeways With Special Lanes. *Transportation Research Part B*, Vol. 31B, No. 2, April 1997, pp. 83-102.
3. Klar, A. and R. Wegener. Vehicular Traffic: From Microscopic to Macroscopic Description. *Transport Theory and Statistical Physics*, Vol. 29, No. 3-5, 2000, pp. 479-493.
4. Kuhne, R.D. and M. B. Rodiger. Macroscopic Simulation Model for Freeway Traffic With Jams and Stop-Start Waves. *1991 Winter Simulation Conference Proceedings*, IEEE, 8-11 December 1991, Phoenix, Arizona, USA, pp.762-770.
5. Shvetsov, V. and D. Helbing. Macroscopic Dynamics of Multilane Traffic. *Physical Review E*, Vol. 59, No. 6, June 1999. pp. 6328-6339.
6. Krauss, S., P. Wagner, and C. Gawron. Metastable States in a Microscopic Model of Traffic Flow. *Physical Review E*, Vol. 55, No. 5, Pt. A, May 1997, pp. 5597-5602.
7. Benz, T. The Microscopic Traffic Simulator AS (Autobahn Simulator). *Proceedings of the 1993 European Simulation Multiconference SCS*, 7-9 June 1993, Lyon, France, pp. 486-489.
8. Emmerich, H. and E. Rank. An Improved Cellular Automaton Model for Traffic Flow Simulation. *Physica A*, Vol. 234, No. 3-4, 1 January 1997, pp. 676-686.

9. Nagel, K., D.E. Wolf, P. Wagner, and P. Simon. Two-lane Traffic Rules for Cellular Automata: A Systematic Approach. *Physical Review E*, Vol. 58, No. 2, August 1998, pp. 1425-1437.
10. Saito, T., K. Yasui, S. Fujii, and S. Itakura. Development of Microscopic Simulation Model for Traffic Network (MICSTRAN-II) and Traffic Flow Simulator For Evaluation of Traffic Signal Control. *Proceedings of the Second World Congress on Intelligent Transport Systems*, Yokohama, Japan, 1995, Vol. 4, pp. 1920-1925.
11. Qi Yang, and H. N. Koutsopoulos. "A Microscopic Traffic Simulator for Evaluation of Dynamic Traffic Management Systems." *Transportation Research Part C*, Vol. 4C, No. 3, June 1996, pp. 113-129.
12. Goles, E. and S. Martinez. *Neural and Automata Networks*. Kluwer Academic Publishing, London, 1990.
13. Schadschneider, A. The Nagel-Schreckenberg model revisited. *European Physical Journal B*, Vol. 10, No. 3, August 1999, pp. 573-582.
14. SMARTTEST Partnership. Final Report SMARTTEST Contract No: RO-97-SC.1059, University of Leeds, Great Britain, 2000.
15. Amin, S.M., A.P. Liu, K. Rink, and E.Y. Roudin. Traffic Prediction and Management via RBF Neural Nets and Semantic Control. *Computer Aided Civil and Infrastructure Engineering*, Vol. 13, No. 5, 1998, pp. 315-327.
16. Nagel, K., and M. Schreckenberg. A Cellular Automaton Model for Freeway Traffic. *Journal de Physique I*, Vol. 2, No. 12, December 1992, pp. 2212-2229.